New Astronomy Reviews 90 (2020) 101545

Contents lists available at ScienceDirect

New Astronomy Reviews

journal homepage: www.elsevier.com/locate/newastrev

INTEGRAL view of AGN

Angela Malizia[*,a], Sergey Sazonov[b], Loredana Bassani[a], Elena Pian[a], Volker Beckmann[c], Manuela Molina[a], Ilya Mereminskiy[b], Guillaume Belanger[d]

[a] OAS-INAF, Via P. Gobetti 101, 40129 Bologna, Italy
[b] Space Research Institute, Russian Academy of Sciences, Profsoyuznaya 84/32, 117997 Moscow, Russia
[c] Institut National de Physique Nuclaire et de Physique des Particules (IN2P3) CNRS, Paris, France
[d] ESA/ESAC, Camino Bajo del Castillo, 28692 Villanueva de la Canada, Madrid, Spain

ARTICLE INFO

Keywords:
INTEGRAL
AGN
Seyferts
Blazars

2010 MSC:
00-01
99-00

ABSTRACT

AGN are among the most energetic phenomena in the Universe and in the last two decades *INTEGRAL*'s contribution in their study has had a significant impact. Thanks to the *INTEGRAL* extragalactic sky surveys, all classes of soft X-ray detected (in the 2-10 keV band) AGN have been observed at higher energies as well. Up to now, around 450 AGN have been catalogued and a conspicuous part of them are either objects observed at high-energies for the first time or newly discovered AGN. The high-energy domain (20-200 keV) represents an important window for spectral studies of AGN and it is also the most appropriate for AGN population studies, since it is almost unbiased against obscuration and therefore free of the limitations which affect surveys at other frequencies. Over the years, *INTEGRAL* data have allowed to characterise AGN spectra at high energies, to investigate their absorption properties, to test the AGN unification scheme and to perform population studies. In this review the main results are reported and *INTEGRAL*'s contribution to AGN science is highlighted for each class of AGN. Finally, new perspectives are provided, connecting *INTEGRAL*'s science with that at other wavelengths and in particular to the GeV/TeV regime which is still poorly explored.

1. INTRODUCTION

Active Galactic Nuclei (AGN) are one of the most powerful phenomena in the Universe. After many decades of observations and studies, our knowledge of these objects has made enormous leaps forward. These galaxies are defined active because they have in their centre an accreting supermassive black hole (SMBH) of masses higher than $M_{\odot}$which radiates across the entire electromagnetic spectrum, from the radio up to gamma-rays. Accretion, i.e. the extraction of gravitational energy from matter infalling onto a black hole, is in fact the most efficient bulk mass-energy conversion process known. The accreting matter orbits around the black hole and, having some angular momentum, through dissipation of energy, flattens to form a disc where magnetic viscosity transfers the angular momentum outward and the mass inward; the accretion disc together with the central black hole makes up the central engine of an AGN.

It is likely, whether the accretion rate is high or low, that the gravitational energy liberated by this process is radiated locally with a large fraction in the form of thermal radiation from the surface of the disc, peaking in the optical/UV bands. A significant amount of these optical/UV photons are reprocessed by a) dust located beyond the sublimation radius and re-emitted in the infrared band (IR); and b) by a corona of hot electrons close to the accretion disc that up-scatters them via inverse Compton in the soft/hard X-ray bands where AGN emit a non negligible fraction of their luminosity (Maraschi and Haardt, 1997; Zdziarski, 1998).

However, disc and corona are just the inner part of the nucleus of an AGN, and the proof that a complex environment surrounds this region is that a large fraction of the radiation may be absorbed by interstellar gas and dust close to the accretion disc and likely re-radiated in other wavelengths. In the classical picture of an AGN, surrounding the accretion disc and the hot corona on 0.01–0.1 parsec scale, there is a region of high velocity gas of 1000 – 5000 km/s, usually referred to as the Broad Line Region (BLR), which determines permitted and intercombination broad emission lines in the optical spectra and can cause ionised absorption producing characteristic features in the UV and soft X-ray bands (the so-called warm absorber).

At a distance of 1-100 pc from the BH is located an obscuring optically thick torus of gas and dust. Whether we consider this torus as dusty-compact or dusty-cloudy, it is the main structure responsible for the absorption of the primary continuum; it can be so thick that it completely hides the primary emission up to several keV.

* Corresponding author.
E-mail address: angela.malizia@inaf.it (A. Malizia).

https://doi.org/10.1016/j.newar.2020.101545
Received 11 December 2019; Received in revised form 2 September 2020; Accepted 6 September 2020
Available online 22 October 2020
1387-6473/

Going to distances greater than 100 pc up to kpc scales, a biconical shaped and highly structured region of lower velocity gas (<900 km/s), the so-called the Narrow Line Region (NLR), is located; radiation which passes through this region produces permitted, intercombination and forbidden narrow lines in the optical-UV band.

Finally, the interaction between the supermassive black hole's rotating magnetic field and the accretion disc can also create powerful magnetic jets that eject material perpendicular to the disc at relativistic speeds and extend for hundreds to thousands of parsecs.

All these ingredients have contributed over the years to explain a wide variety of AGN classes at all wavebands and led to the postulation of the Unified Theory of AGN (Antonucci et al., 1993; Urry and Padovani, 1995) which in its simplest version hypothesises that the diversity of AGN can be largely explained as a viewing angle effect, although also accretion rate and efficiency play an important role.

A main ingredient of this orientation-based model is the absorbing material, principally the optically and geometrically thick torus, which obscures the nuclear regions of an active galaxy (the accretion disc and the hot corona as well as the BLR). We optically classify an AGN as type 2 or type 1 depending on whether our line of sight intercepts or not this obscuring material. Furthermore, we classify an AGN as radio loud or radio quiet if its emission at radio frequencies is either strong or weak. Within the radio-loud class, differences in typologies (BL Lac objects, Flat Spectrum Radio Quasars and Radio Galaxies) have also been explained in terms of orientation, i.e. referring to one or the other type if the jet axis is perfectly aligned with the observer's line of sight or progressively misaligned.

What clearly emerges from this AGN complex structure is that absorption is a key ingredient to understand the physics of these objects. For this reason, the hard X-ray band is the most appropriate for AGN population studies since it is almost unbiased[1] against obscuration and therefore free of the limitations which affect surveys at other frequencies, i.e. from optical to soft X-rays.

Furthermore, the hard X-ray band represents an important window for spectral studies of AGN. The continuum of active galaxies in the X-ray band is well explained by the Comptonisation process which is described by a power law of photon index (Γ) in the range 1.5 – 2 showing an exponential cut-off (E_c) at around 100 keV. Reprocessing of X-ray photons from the surface of the disc, or from more distant material, can produce in addition to fluorescent emission lines, also a hump at 20-30 keV due to Compton reflection. Therefore high-energy data are crucial to estimate the slope of the continuum emission over a wide energy band but also to measure the high energy cut-off and the reflection fraction. These are important parameters because they enable us to understand the physical characteristics and the geometry of the region around the central nucleus. In other words, in the framework of the disc-corona system, while the cut-off energy is related essentially to the temperature kT_e of the electrons in the corona, a combination of the temperature and optical depth, τ, of the scattering electrons determines the spectral slope. Thus simultaneous measurements of Γ and E_c allow us to understand the physical parameters of the Comptonising region. Therefore, the more accurate are the measurements of these parameters, the better we can determine the geometry and the physical properties of the inner region of AGN.

Finally, high-energy data provide also important information about the AGN contribution to the cosmic X-ray background (CXB). While the fraction of the CXB resolved into discrete sources is ~ 80% (Luo et al., 2017), ~ 90% (Luo et al., 2017), ~ 60% (Ranalli et al., 2013) and ~ 35% (Harrison et al., 2016) in the 0.5–2, 2–7, 5–10 and 8–24 keV energy bands, respectively, it becomes much lower (see section 4.4) at higher energies, near the peak of the CXB spectral intensity at around 30 keV. In order to reproduce the shape of the CXB, synthesis models (e.g., Comastri et al. (2006)) need to use several parameters, such as the fraction of heavily obscured sources (the so-called Compton thick AGN characterised by $N_H \geq 10^{24} cm^{-2}$), the coverage and the geometry of the cold gas distributed around the black hole responsible for the reflection hump, the photon index and high-energy cut-off of the primary continuum emission as well as the luminosity function in the energy range of interest. Therefore, the determination of such parameters, in particular photon indices and cut-off energies, their mean values, and their distributions over a wide sample of sources, covering a broad range of energies (above 100 keV), is essential to obtain a much firmer estimate of the AGN contribution to the CXB at high energy.

In the last decades both *INTEGRAL*/IBIS (Barthelmy et al., 2005) and *Swift*/BAT (Barthelmy et al., 2005), having good sensitivity and wide-field sky coverage, were able to make significant progress in the study of the high-energy domain (20-200 keV). In particular they have provided a great improvement in our knowledge of the high-energy extragalactic sky by detecting more than 1000 (mostly local) AGN at energies above 15 keV. It is worth noting that, due to the observational strategy, *INTEGRAL* plays a key role in detecting new absorbed objects and in particular AGN along the Galactic Plane, while *Swift*/BAT is more effective at higher Galactic latitudes. This makes the two observatories fully complementary also in the case of extragalactic studies.

In this work we will review the contribution of *INTEGRAL* and in particular of the imager IBIS to AGN science, highlighting the most important results reached in its 17 years in orbit.

2. From first detections to AGN catalogues

As mentioned before, the most important application of *INTEGRAL* has been for finding hard X-ray emitting sources along the Galactic Plane. The so-called "Zone of Avoidance" refers to the area comprised between ±10-15°,above and below the Galactic plane. Gas and dust obscure starlight within this region and screen nearly all background extragalactic objects from traditional optical-wavelength surveys; in the optical, as much as 20%of the extragalactic sky is obscured by the Galaxy. As a consequence, historically the Galactic Plane has not been a focus for extragalactic astronomy. Hard X-rays (10 keV) are however able to penetrate this zone providing a window that is virtually free of obscuration relative to optical wavelengths and partly also to soft X-rays.

The hard X-ray band has been poorly explored before the *INTEGRAL* and *Swift* satellites and the only previous truly all-sky survey conducted, dates back to the eighties. This pioneering work, made with the *HEAO1*-A4 instrument (Levine et al., 1984), yielded a catalogue of about 70 sources down to flux level of typically 1/75 of the Crab (or 2-3 $\times 10^{-10}$erg $cm^{-2}s^{-1}$) in the 13-80 keV band. Only 7 extragalactic objects were reported in this survey: none of these objects is within 10°of the Galactic Plane and only two (Centaurus A and the Perseus cluster) are located below 20°in Galactic latitude. Pointed observations by *BeppoSAX*/PDS (Frontera et al., 1997) have unveiled more sources but observations were sometime limited by the non imaging capability of the high energy instrument (PDS) which is particularly crucial in the Galactic Plane region.

A decisive step forward in the exploitation of the entire hard X-ray sky has been possible thanks to the imager IBIS on board *INTEGRAL*, which since the beginnings of the mission, allowed the detection of AGN with a sensitivity up to a few mCrab in the most exposed regions (i.e. the Galactic centre) with an angular resolution of 12 arcmin and a point source location accuracy of 2-3 arcmin (Bassani et al., 2004b).

The capabilities of *INTEGRAL*/IBIS in studying extragalactic sources, were revealed soon after the launch of the satellite and in particular during the Core Programme which lasted for the first five years of the mission and consisted of 45 - 35% of the total observing time. The Core Program (CP) was dedicated to key investigations and

[1] Note that only objects with $N_H > 10^{24} cm^{-2}$could be missed in these surveys due to their much dimmer flux which prevents detections by current hard X-ray telescopes

devoted to regular surveys of the Galactic Plane and selected deep sky fields at high galactic latitudes. By observing around 9000 square degrees of the sky, the CP allowed the detection of a dozen AGN as well as a quite large number of new unidentified objects firstly detected at high energies. Most of these firstly detected AGN were bright Seyfert 2 systems, i.e. absorbed objects, 3 of which were Compton thick, all located in the Galactic Plane (Bassani et al., 2004a; Soldi et al., 2006; Bassani et al., 2004b). Many of these AGN have been previously studied at energies above 20 keV and for them *INTEGRAL* largely confirmed previous findings. Among these, there is also the first blazar detected by *INTEGRAL*: PKS 1830-211 at a relatively high redshift ($z = 2.507$) (Bassani et al., 2004b).

Furthermore, IBIS/ISGRI data of the brightest AGN have been used alone or in conjunction with soft 2–10 keV data to perform dedicated studies (Sazonov, Revnivtsev, Lutovinov, Sunyaev, Grebenev, 2004; Beckmann et al., 2005) exploring their spectral characterisation.

It became soon evident that the population of AGN emitting above 20 keV was growing thanks to the discovery that many of the new detections were indeed active galaxies.

The first IBIS survey (Bird et al., 2004), based on the first year of *INTEGRAL* observations, counted only 5 AGN which became 33 (almost 20% of the entire catalogue) in the second survey (Bird et al., 2006). A couple of dedicated AGN surveys were published by Beckmann et al. (2006) and Bassani et al. (2006) which listed 42 and 66 sources respectively. Both surveys highlighted the capability of *INTEGRAL* to probe the extragalactic high energy sky and most of all to find new and/or absorbed active galaxies. Since 2004, a sequence of IBIS all-sky survey catalogues (Bird et al., 2004; 2006; 2007; 2009; 2016) based on data from the ISGRI detector have been published at regular intervals, making use of an ever-increasing data set as new observations become publicly available. The last edition of the IBIS all sky survey (Bird et al., 2016) lists 939 sources: is clearly visible from Figure 1, the majority of these sources are AGN and newly discovered (i.e. those with an IGR designation) sources which, in large part, are expected to be AGN after proper follow up. On the other hand, also deep extragalactic surveys have been produced over the years thanks to long pointings at specific sky areas such as the Large Magellanic Cloud (Grebenev et al., 2012; Mereminskiy et al., 2016), the 3C 273/Coma and M81 regions (Bikmaev, Sunyaev, Revnivtsev, Burenin, 2006; Mereminskiy et al., 2016). Figure 2 taken from Mereminskiy et al. (2016), shows these three fields (M81 (exposure of 9.7 Ms), Large Magellanic Cloud (6.8 Ms) and 3C 273/Coma (9.3 Ms)) in the 17-60 keV band as seen by *INTEGRAL*/IBIS after 12 years (2003-2015) of observations.

As the total number of known or newly discovered AGN grew, it was possible to assemble them for population studies as done over the years by Malizia et al. (2012) and Malizia et al. (2016). So far the number of AGN listed in this dataset amounts to more than 400 objects.

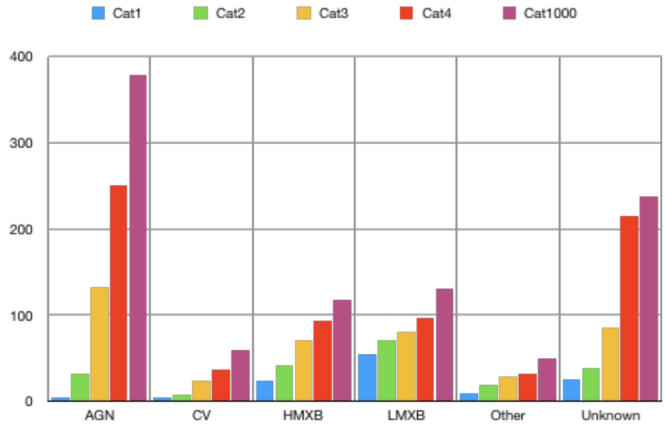

Fig. 1. Evolution of source type and number through the five *INTEGRAL* IBIS/ISGRI catalogs produced to date (courtesy of A. J. Bird)

It is also worth mentioning here the IBIS high energy catalogues i.e. those collecting sources detected above 100 keV. There were 10 AGN listed in Bazzano et al. (2006) and 28 AGN in Krivonos et al. (2015), 7 of which detected also in the 150–300 keV band. Furthermore, a catalogue produced in 2008 by Bouchet et al. (2008) based on SPI (the other primary wide field instrument on *INTEGRAL*) data, reported 34 AGN, 10 of which detected up to 200 keV and 4 in the 200–600 keV band.

As mentioned above *INTEGRAL* gave a fundamental contribution in finding new high energy emitters, their number increasing more and more along surveys. The *INTEGRAL* community made a huge effort in the identification and classification of these new IGR sources. This led to the discovery of new AGN as well as of new classes of objects emitting at high-energies. However, the classification of a new, high-energy detected source is by no means trivial. First of all, one has to reduce the positional uncertainty associated with the high energy detection, which in some cases can be as high as 4–5 arcminutes. To do this, 2-10 keV data are important because they provide a unique tool to associate the high energy source with a single/multiple X-ray counterpart/s. When archival observations were not available, follow-up campaigns have been performed with all X-ray instruments such as *XMM, Chandra* and *Swift*/XRT which allowed also the spectral characterisation of the sources (Boettcher (2010); Malizia et al., 2007; Sazonov et al., 2008b; Landi et al., 2010; Landi et al., 2017).

Association of the X-ray source with an object detected at other wavelength is a fundamental step in the analysis as it allows to pinpoint the correct counterpart, locate it with arcsec accuracy and therefore provide a way to study the source at other wavelengths. Optical, IR or radio catalogues are then searched in order to find the appropriate classification of the object. If this search does not yield any result, follow-up observations, above all in the optical, are then planned and carried out.

A parallel effort regarding the spectroscopic identification of newly-detected or poorly studied hard X-ray sources has been performed by several groups worldwide soon after the publication of the 1st IBIS survey.

To this date, this task has allowed the determination of the nature of around 150 AGN, with nearly 60% of them classified as broad emission line nuclei. The bulk (~90%) of these identifications stemmed from the program of Masetti and collaborators which encompassed the use of at least a dozen telescopes across the globe (see Bruni et al., 2019 >) and references therein). Further AGN identifications from other groups have also been reported in the literature like in Bikmaev et al. (2006, 2008); Zurita Heras et al. (2009); Chevalier et al. (2019)). It is worth noting that an overlap of detected sources is present across the *INTEGRAL*and *Swift*/BAT (e.g. Oh et al. (2018)) catalogues. Therefore, several identifications of *Swift*hard X-ray emitters may be also accommodated in the *INTEGRAL* surveys (e.g., Collmar et al. (2010)) and references therein; Karasev et al. (2018)). Thus, the total number of identifications reported above should actually be considered as a strict lower limit.

This association/classification method has also been used to construct *INTEGRAL* AGN catalogues and so guarantees that all objects in these catalogues are fully characterised in terms of optical identification/classification as well as fully studied in terms of X-ray spectral properties.

3. AGN Types and Population studies

The total number of AGN so far detected by *INTEGRAL*, including recent additions, amounts to 440 objects. In Figure 3 their 20–100 keV observed luminosity is plotted against redshift, differentiating objects in three main optical classes: broad line AGN (red filled squares), narrow line AGN (gold filled circles) and blazars (blue stars). The luminosities have been calculated for all sources assuming $H_0 = 69.6$ km $s^{-1}Mpc^{-1}$and $q_0 = 0$.

We find that the source redshifts span a range from 0.00084 to 3.7

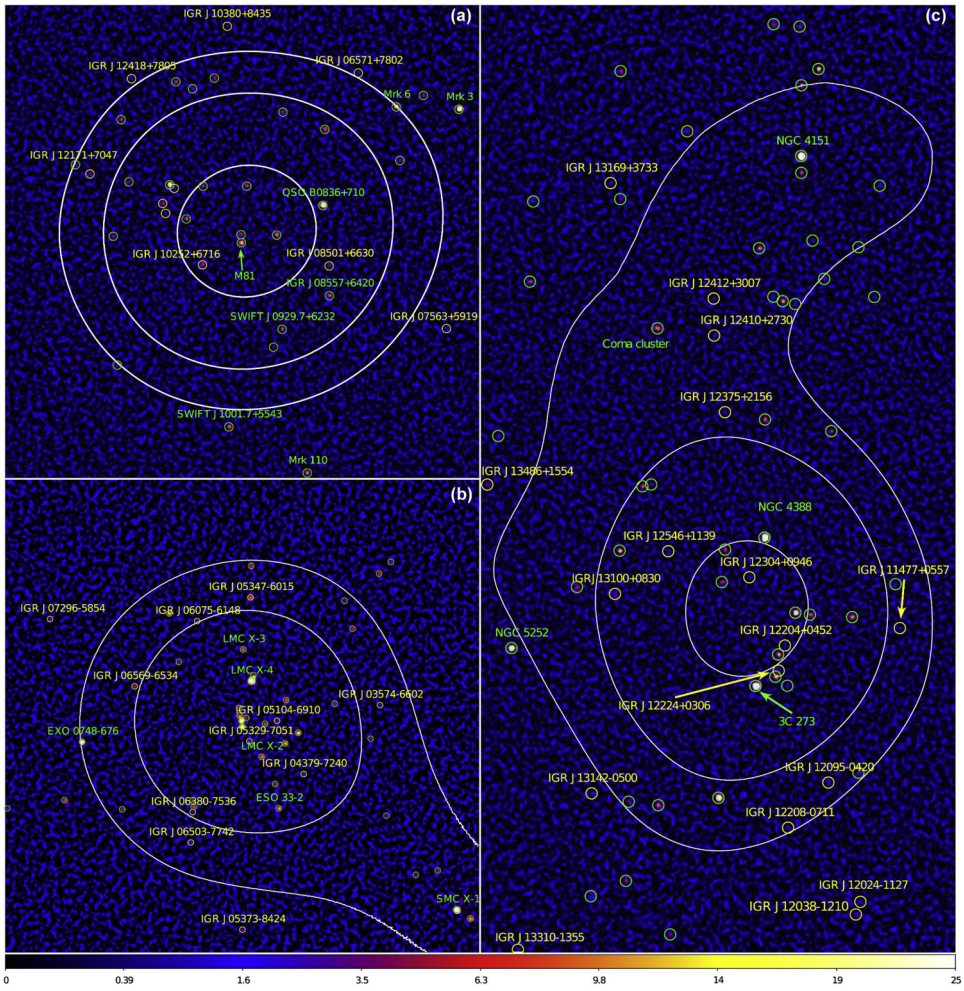

Fig. 2. Hard X-ray maps of the M81, LMC and 3C 273/Coma fields as in Mereminskiy et al. (2016)

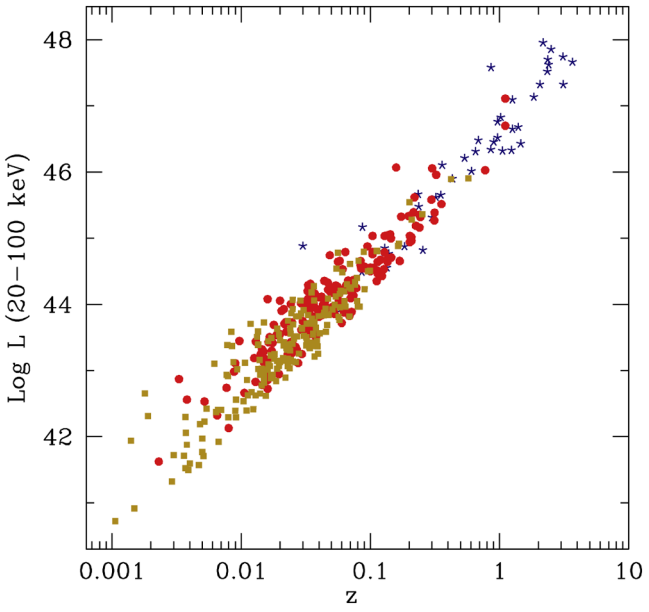

Fig. 3. Observed hard X-ray (20-100 keV) luminosity versus redshift for the whole *INTEGRAL* AGN sample. Gold filled circles are narrow line AGN, red filled squares are broad line AGN and blue stars are balzars.

with a median of $z = 0.035$, while the Log of 20-100 keV luminosities in ergs s^{-1}(assuming isotropic emission) ranges from 40.23 to ~48 with a mean at around 44. M81 (a Seyfert 1.8/LINER) is the closest and least luminous AGN seen by *INTEGRAL*, while IGR J22517 + 2218 (a broad line QSO) is the farthest and most luminous object so far detected; the former hosts a black hole of mass $M = 7 \times 10^7 M_\odot$while the latter houses a more massive one ($M = 10^9 M_\odot$,Lanzuisi et al. (2012)). *INTEGRAL*also detected NGC 4395, a Seyfert 2 galaxy which hosts a black hole of about $10^4 M_\odot$; this mass has recently been estimated through reverberation mapping of the broad line region and resulted to be among the smallest central black hole masses ever reported for an AGN (Woo et al., 2019). In conclusion, the *INTEGRAL*sample spans a large range in source parameters and is therefore representative of the population of AGN selected in the hard X-ray band.

After 17 years of *INTEGRAL* surveying the extragalactic sky, we can now say that all classes of AGN that are seen in the 2-10 keV band, are also detected at higher energies. In the pie chart of Figure 4 the main classes seen by *INTEGRAL* are highlighted: it is evident from the figure that a large fraction is made up of Seyfert galaxies, equally divided in type 1 and 2; the second most numerous class is that of blazars, followed by a small number of objects of other classifications which are also interesting to study. The large database accumulated, allowed over the years to probe new AGN classes, to investigate the absorption properties of active galaxies, to test the AGN unification scheme and to perform population studies.

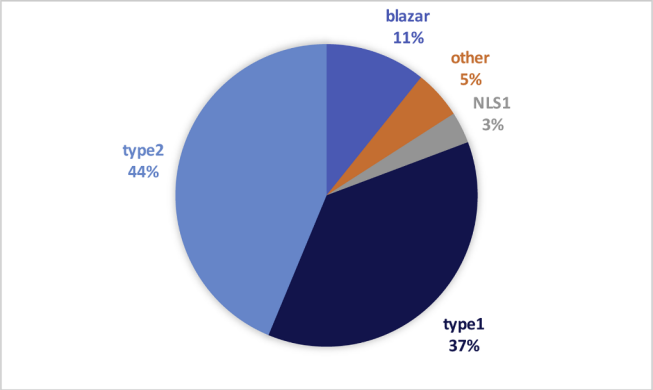

Fig. 4. Pie chart of the main classes of AGN in the *INTEGRAL* sample.

For example *INTEGRAL* has detected for the first time at high energies Narrow Line Seyfert 1 galaxies (NLS1) (Malizia et al., 2008). These are interesting targets as they are characterised by unique properties when compared to their broad line analogues, both in the optical (see e.g. Osterbrock and Pogge (1985)) and in the X-rays, where they show stronger variability (both in flux and spectral shape) and steeper power law spectra. The most widely accepted explanation for these differences is that NLS1 have smaller black hole masses than normal Seyfert 1s; however their luminosities are comparable (Pounds et al., 1995), suggesting that they must be emitting at higher fractions of their Eddington luminosity and therefore should also have higher fractional accretion rates. A plausible scenario suggests that black holes in NLS1 have not yet been fed enough to become massive and are in a rapidly growing phase (Mathur, 2000); if NLS1 are indeed in an early phase of black hole evolution, then they are key targets for the study of AGN formation and evolution. Within the INTEGRAL AGN sample only 15 objects are classified as NLS1 (or 3%of the sample). Most of these objects have been studied in detail by Panessa et al. (2011)who found that hard X-ray selected NLS1 show variability over a broad range of X-ray frequencies, lack a strong soft excess, and often display fully or partially covering absorption. As expected, NLS1 detected at high energies by *INTEGRAL* are also associated to small black hole masses and occupy the lower tail of the Eddington ratios distribution with respect to classical NLS1.

Another interesting type of AGN first detected in hard X-rays by *INTEGRAL* are the XBONGs, i.e. X-ray Bright Optically Normal Galaxies (Comastri et al., 2002) which are bright in X-rays (X-ray luminosity of 10^{43}-10^{44}erg s^{-1}) but are optically dull, i.e. they are hosted by normal galaxies whose optical spectra show no emission lines. Over the years, XBONG have shown to be a mixed bag of objects primarily including normal elliptical galaxies and AGN whose optical nuclear spectrum is probably diluted by the strong stellar continuum. *INTEGRAL*XBONG (6 detected so far) are all heavily absorbed in X-rays (Log Nfrom 23 to more than 24 cm^{-2}) and are quite bright above 20 keV (L_{20-100}keV in the range 10^{42}– 10^{44}erg s^{-1}). These are luminosities typical of AGN which implies that *INTEGRAL*can detect heavily absorbed objects whose hosting galaxy outshines the active nucleus; these AGN would normally be missed in optical surveys.

Equally absorbed and bright are the majority of LINERs (Low-Ionization Nuclear Emission Regions) seen by *INTEGRAL* and in fact many of them are classified as LINERs of type 2 i.e. showing only narrow lines in their optical spectra. There are 20 LINERs in the *INTEGRAL* AGN sample and only 2 are of type 1, i.e. unabsorbed. Also LINERs have been detected at high energies for the first time by *INTEGRAL* (first identifications by Masetti et al. (2008b)), clarifying the controversial origin (AGN versus starburst) of the ultimate power source of these objects. Given their high 20-100 keV luminosities, it is almost certain that all *INTEGRAL* LINERs are powered by an AGN, even if their mean luminosity (~1.7 $\times 10^{43}$erg s^{-1}) is slightly lower than that of classical Seyfert galaxies (~5.5 $\times 10^{43}$erg s^{-1}). The result that emerged by the *INTEGRAL*studies (Malizia et al., 2012), is that LINERs are numerous as a class and like Seyfert galaxies, come in two flavours: unabsorbed type 1 and absorbed type 2, with *INTEGRAL*having the capability of detecting the second type in large numbers.

Regarding population studies, Beckmann et al. (2009) first used a sample of *INTEGRAL* detected AGN to study source parameters on a large scale. An interesting result that emerged from this study is the significant correlation found between the hard X-ray and optical luminosity and the mass of the central black hole in the sense that more luminous objects appear also to be more massive. This finding allowed to construct a black hole fundamental plane similar to the one found using radio data ($L_V \propto L_X^{0.6} M_{BH}^{0.2}$).

The accurate study, at optical and X-rays frequencies of all *INTEGRAL* AGN has also allowed the study of the correlation between optical classification and X-ray absorption thus allowing to perform a strong test on the AGN unification model. Although the presence of a correlation is expected and indeed found, i.e. type 1 AGN are typically unabsorbed while type 2 AGN are often absorbed, the strength of the correlation is never 100%. Using a large sample of *INTEGRAL* AGN, Malizia et al. (2012) have found that only a small percentage of sources (12.5%) does not fulfil the expectation of the Unified Theory and looking in depth at these outliers concluded that the standard-based AGN unification scheme is followed by the majority of bright AGN. The only outliers are absorbed type 1 AGN characterised by complex X-ray absorption likely due to ionised gas located in an accretion disc wind or in the biconical structure associated to the central nucleus and so unrelated to the torus. The other outliers are type 2 AGN which do not show X-ray absorption but this could be either due to variability (meaning that their different optical/X-ray classifications can be explained in terms of state transitions and/or non simultaneous X-ray and optical observations) or to a high dust-to-gas ratio.

Finally, Panessa et al. (2015) studied the radio properties of a complete sample of *INTEGRAL* detected AGN, found a significant correlation between the radio flux at 0.8/1.4 GHz and the 20-100 keV flux, with a slope between these two parameters consistent with that expected for radiatively efficient accreting systems. This indicates that the high-energy emission coming from the inner accretion regions correlates with the radio emission averaged over hundreds of pc scales (i.e., thousands of years).

4. Main Results: Seyfert galaxies

4.1. Broad Band studies and high energy cutoff

The study of the X/hard-X ray emission of AGN, i.e. from 2 keV to ≥100 keV, is a fundamental tool in order to have a direct probe of their innermost regions. As said before, the primary continuum over this broad band can be roughly represented by a cut-off power law produced by the Comptonisation mechanism which is believed to arise in the corona, close to the central super-massive black hole. Clearly to have an overview of the physics and structure of the corona we need to study the broad-band spectra of a large sample of AGN in order to account for all spectral components, remove the degeneracy between parameters and therefore being able to obtain a precise estimate of the photon index and high-energy cut-off for a large number of objects. These two parameters are, as said, strictly linked to the temperature and the optical depth of the corona (Petrucci et al., 2001).

Before *INTEGRAL* and *Swift*/BAT, broad band spectra were available only for a limited number of bright AGN, basically due to the scarcity of measurements above 10-20 keV, with most of the information coming from broad-band spectra provided by the *BeppoSAX* satellite which had a broad energy coverage (0.1-100 keV) but no imaging capability above 10 keV. Analysis of *BeppoSAX* data of types 1 and 2 AGN (Perola et al., 2002; Dadina, 2007; Malizia et al., 2003) gave evidence for a wide range of values for the cut-off energy, ranging from 30 to 300 keV and

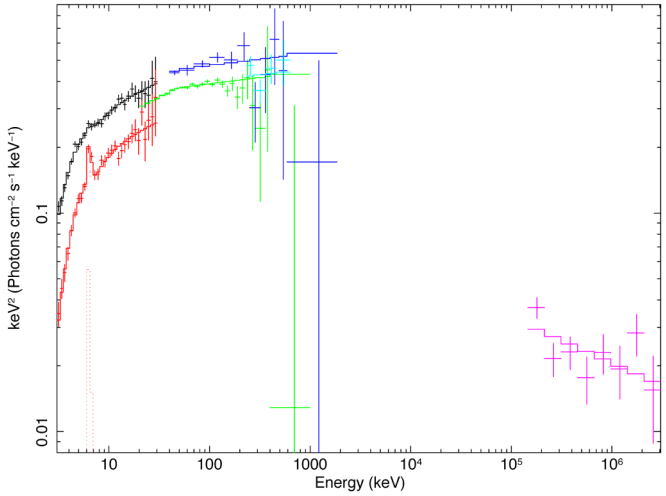

Fig. 5. Combined *INTEGRAL* and (non-simultaneous) *Fermi*/LAT unfolded spectrum of Cen A as in Beckmann et al. (2011). The data are modelled by a double broken power-law with individual normalisation for the data of different epochs. The highest energy bins for IBIS/ISGRI and SPI are only upper limits.

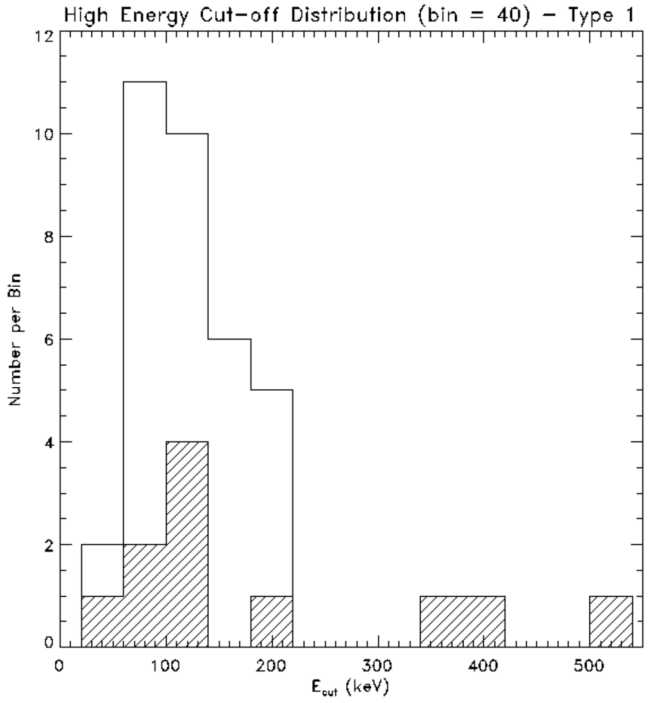

Fig. 6. High-energy cut-off distribution of the entire sample from Malizia et al. (2009). The diagonally hatched histogram represents sources for which only lower limits of E_c are available.

higher, and an apparent different distribution of photon index and reflection parameter in different classes of AGN, e.g. Malizia et al. (2003).

Spectral parameters of a few individual local bright AGN have been measured using *INTEGRAL* data with the addition of very high energy data as in the case of Cen A (Beckmann et al., 2011), see Figure 5. More sources have been studied using *INTEGRAL* data in conjunction with those of other X-ray satellites, mainly *Swift*/XRT and *XMM-Newton*, e.g. NGC 4151 (Lubiński et al., 2010), NGC 4388 (Beckmann et al., 2004), NGC 2110 (Beckmann and Do Cao, 2010), NGC 4945 (Fedorova and Zhdanov, 2016) and many others.

Spectral studies have also been performed for the first time for AGN located in the Galactic Plane such as for GRS 1734-292 and other 6 objects as in Molina et al. (2006). Furthermore, thanks to the good statistical quality of the *INTEGRAL* data, for these local AGN, flux variability and spectral changes have been studied for the first time for many of them (e.g. Soldi et al. (2008); Fedorova and Zhdanov (2016); Molina et al. (2013)). Although snapshot observations in the soft X-rays (typically from *XMM-Newton* or from *Swift*/XRT) and time-averaged (on timescales of years) measurements at high energies are not contemporaneous and acquired differently, the match between the two is generally good, with the cross-calibration constant between the two instruments being typically around 1 (Panessa et al., 2008; de Rosa et al., 2012; Molina et al., 2013; Fedorova et al., 2011). Broad-band spectral analysis of the brightest Setyfert 1 galaxies as in Panessa et al. (2008) and Seyfert 2 as in de Rosa et al. (2012), have also been performed defining the characteristics of the two classes on quite large samples of objects.

The broad-band spectral analysis of 41 Seyfert 1 galaxies belonging to the *INTEGRAL* complete sample (Malizia et al., 2009) performed by fitting together *XMM, Swift*/BAT, and *INTEGRAL*/IBIS data in the 0.3–100 keV energy band allowed Malizia et al. (2014) to confirm the distribution of photon indices ($\Gamma = 1.73$ with standard deviation of 0.17) and, for the first time, to provide the high-energy cut-off distribution for a large sample of objects. Malizia et al. (2014)found that the mean high energy cut-off was 128 keV with a spread of 46 keV (see Figure 6), clearly indicating that the primary continuum typically decays at much lower energies than previously thought. This value is more in line with the synthesis models of the cosmic diffuse background, which often assume an upper limit of ~200 keV for the cut-off (Gilli et al. (2007), see also section 4.4).

In Malizia et al. (2014) the main parameters of the primary continuum have been estimated by employing a baseline phenomenological model (`PEXRAV` model in `XSPEC`) composed of an exponentially cut-off power-law reflected from neutral matter. At soft energies, when required by the data, intrinsic absorption in terms of simple or/and complex, cold or ionised absorbers have been added and when spectra showed clear signs of a soft excess, this has been generally fitted with a thermal component. A gaussian line has also been included, to take into account the presence of the iron kαline at around 6.4 keV; and when present residuals around 7 keV, these have also been fitted adding a second gaussian line to take into account the iron kβfeature.

With these spectral parameters Malizia et al. (2014), following Petrucci et al. (2001), have been able to evaluate the actual physical parameters of the Comptonising region by assuming the plasma temperature to be $kT_e = E_c/2$, for optical depth τless or ~1, and $kT_e = E_c/3$ for $\tau \gg 1$. The most probable range of plasma temperatures kT_ederived from this study was found to be in the range 20 to 100 keV (or 2 - 12 $\times 10^8$ K). Assuming the average value of $\Gamma = 1.73$ and taking into account both low and high values of E_c,acceptable solutions for τin the range 1 to 4 have been obtained. These results are in good agreement with those previously found by Petrucci et al. (2001)for a small sample of Seyfert 1 galaxies with *BeppoSAX* observations, and by Beckmann et al. (2009) applying a cut-off power law model to the stacked JEM-X plus IBIS spectral data of Seyfert 1 ($E_c = 86^{+21}_{-14}$keV).

Furthermore, the high energy cut-off distribution of the *INTEGRAL* complete sample of type 1 AGN is in good agreement with what found by Lubiński et al. (2016) employing a more physical model (`COMPPS` model) on a sample of 28 bright AGN (type 1 and 2) and analysing *INTEGRAL* data together with soft X-ray ones acquired by *XMM-Newton, Suzaku* and *RXTE*. Lubiński et al. (2016) tested several model options assuming a thermal Comptonisation of the primary continuum accompanied by a complex absorption and a Compton reflection. They accurately determined the mean temperature of the electron plasma to be 26 ≤kTe ≤62 keV for the majority of the sample objects with only two sources exhibiting temperatures kT_e>200 keV. These low temperatures of the electron plasma obtained in all these studies, imply that the template Seyferts spectra used in the population synthesis models of

AGN should be revised: the most important consequence of a shifted high-energy cut-off will be a considerably smaller fraction of CT AGN needed to explain the peak of the CXB spectrum.

Most of the works mentioned above, made use of non-simultaneous low versus high energy data, and despite the introduction of cross-calibration constants to properly take into account flux variability (and possible mismatches in the instruments calibration), some degree of uncertainty remains since spectral variability cannot be excluded *a priori*. Therefore, if one wants to remove this ambiguity, it is fundamental to have simultaneous observations in both the soft and hard X-ray bands and this is now achievable with *NuSTAR*. In a recent work Molina et al. (2019) presented the 0.5 – 78 keV spectral analysis of 18 broad line AGN belonging to the *INTEGRAL* complete sample, those for which simultaneous *Swift*/XRT and *NuSTAR* observations were available. Employing the same simple phenomenological model to fit the data as in Malizia et al. (2014), these authors found a mean high-energy cut-off of 111 keV ($\sigma =$ 45 keV) for the whole sample, in perfect agreement with what previously found employing *INTEGRAL*data. These findings also confirm that simultaneity of the observations in the soft and hard X-ray band is not essential once flux and spectral variability are properly accounted for.

Finally, compatible values of photon index and cut-off values have been found by Molina et al. (2013) using only high energy data i.e. *INTEGRAL*/IBIS and *Swift*/BAT. Furthermore, this study allowed also a cross-calibration between the two instruments, finding general good agreement between BAT and IBIS spectra, despite a systematic mismatch of about 22 per cent in flux normalisation.

These and other high-energy spectral studies prompted Fabian and collaborators (Fabian et al., 2015; 2017) to propose the pair thermostat model to explain the observations. In the compactness/temperature diagram, AGN coronae which are hot and radiatively compact, are located close to the boundary of the region which is forbidden due to runaway pair production. Pair production and annihilation can be considered essential ingredients in AGN corona physics and strongly affect the shape of the observed spectra. In fact, if photons are energetic enough, the subsequent increase in luminosity produces electron-positron pairs rather than an increase in temperatures, until a point of equilibrium is reached. At this point, pair production consumes all the available energy, therefore limiting the coronal temperature; electron-positron pair production becomes a runaway process thus acting as a sort of thermostat. Pair production from the non-thermal component (hybrid plasma compared to pure thermal plasma) can reduce the temperature leading to a much wider range of values, more consistent with present observations (Fabian et al., 2017).

4.2. Absorption and Compton thick fraction

As said before, an obscuring 'torus' is believed to be responsible for the type 1 and 2 division of Seyfert galaxies and quasars. What is the actual structure of the torus and what is its physical relation to other structural components of AGN such as the accretion disc and broad-line region, is still unclear although progress in understanding this issue has been recently made (Ricci et al., 2017; Hönig, 2019). These are some of the central questions in AGN research and hard X-ray surveys provide a more direct answer than studies at lower energies because these surveys are not affected by absorption bias except for very heavy absorption.

When an X-ray telescope observes an AGN through the torus, the measured spectrum will exhibit a characteristic low-energy cutoff due to the photoabsorption of the soft radiation in the gas and dust of the torus (and perhaps also in the enclosed broad-line region), which allows one to estimate the absorption column density, $N_{\rm H}$,along the viewing direction. A statistical analysis of absorbing columns determined in this way (or by a similar but more model-dependent method for Compton-thick AGN) for a representative sample of objects makes it possible to infer the typical optical depth and covering fraction of the torii in the AGN population. With this understanding, a lot of efforts have been put into follow-up X-ray spectral observations of *INTEGRAL*(and *Swift*) detected AGN (see the previous sections), which has eventually resulted in a unique and well characterised sample of local ($z \lesssim 0.2$) hard X-ray selected AGN.

One of the earliest attempts to use *INTEGRAL* data for AGN absorption studies was undertaken by Beckmann et al. (2006). They made use of a sample of 38 Seyfert galaxies detected by IBIS in the first year of the mission, with absorption information available for 32 of them. Already this limited statistics provided a hint that the fraction of absorbed ($N_{\rm H} > 10^{22}$ cm^{-2}) AGN decreases with increasing hard X-ray (20–40 keV) luminosity. Although the statistical significance of this result was very low, it was consistent with other emerging indications of such a trend both in the local (Sazonov and Revnivtsev, 2004; Markwardt et al., 2005) and distant (Steffen et al., 2003; Ueda et al., 2003) Universe. The Beckmann et al. (2006)sample included 4 Compton-thick ($N_{\rm H} > 10^{24}$ cm^{-2}) objects, all previously known (NGC 1068, Mrk 3, NGC 4945 and Circinus galaxy), implying that the observed fraction of such AGN is ~10% or somewhat higher, taking into account the absence of absorption information for several objects.

Malizia et al. (2007) carried out a statistical analysis of 38 *new* AGN discovered by *INTEGRAL*/IBIS (some of these objects have also been independently found by *Swift*/BAT) and followed up with *Swift*/XRT. Sixteen objects proved to be absorbed AGN and three others were suggested to be Compton-thick based on the low ratios of the observed fluxes in the 2–10 keV and 20–100 keV energy bands. Therefore, the inferred fractions of absorbed and Compton-thick objects (~ 50% and ~ 10%) proved to be in good agreement with the results of Beckmann et al. (2006)despite the largely different samples of AGN (newly discovered vs. mostly previously known objects).

A substantially larger sample of AGN, based on the first three and a half years of observations of the sky with IBIS (Krivonos et al., 2007), was analysed by Sazonov et al. (2007). Specifically, they used a set of 66 Seyfert galaxies located at $|b|>5°$. The enhanced sample provided increased evidence that the fraction of absorbed AGN decreases with increasing luminosity (17–60 keV). The observed fraction of Compton-thick objects was again found to be ~ 10% with an upper limit of ~ 20% (taking into account missing information on the absorption columns for some of the objects).

Later on, several more studies (Malizia et al., 2009; Beckmann et al., 2009; Sazonov et al., 2010; 2015) have taken advantage of the ever increasing catalogue of *INTEGRAL* detected AGN and follow-up efforts to tighten the constraints on the absorption properties of the local AGN population. In particular, using *INTEGRAL* selected AGN, it was assessed for the first time that even at high energy a bias in the estimation of the fraction of Compton thick sources still exists (Malizia et al., 2009). Their flux is reduced due to sensitivity limit, but if corrected their fraction turns out to be of 20%, which is more in line with estimates at other wavebands. Afterwards this results has been confirmed using *Swift*/BAT data (Burlon et al., 2011).

An important step forward has been made by Sazonov et al. (2015) using a sample of 151 local Seyfert galaxies detected in the 17–60 keV energy band by IBIS (at $|b|>5°$), from the 7-year all-sky catalogue of Maiolino and Rieke, 1995;). This sample is highly complete in terms of supplementary information (optical types, distances and X-ray absorption columns) and consists of 67 unabsorbed ($N_{\rm H} < 10^{22}$ cm^{-2}) and 84 absorbed ($N_{\rm H} > 10^{22}$ cm^{-2}) objects including 17 proven or likely Compton-thick ($N_{\rm H} > 10^{24}$ cm^{-2}) AGN (see Figure 7and Semena et al. (2019)). The observed fractions, i.e. without the correction for the absorption bias, of absorbed and Compton-thick objects turned out to be nearly the same (~ 60% and ~ 10%) as in the previous analyses of smaller samples, despite the increased depth of the IBIS survey making it possible to probe a broader (in terms of luminosity and distance) population of AGN. A similar fraction (~ 8%) of Compton-thick AGN is also observed in the *Swift*/BAT survey (Ricci et al., 2015).

Sazonov et al. (2015) decisively ascertained the declining trend of the observed fraction of absorbed AGN with increasing luminosity (see

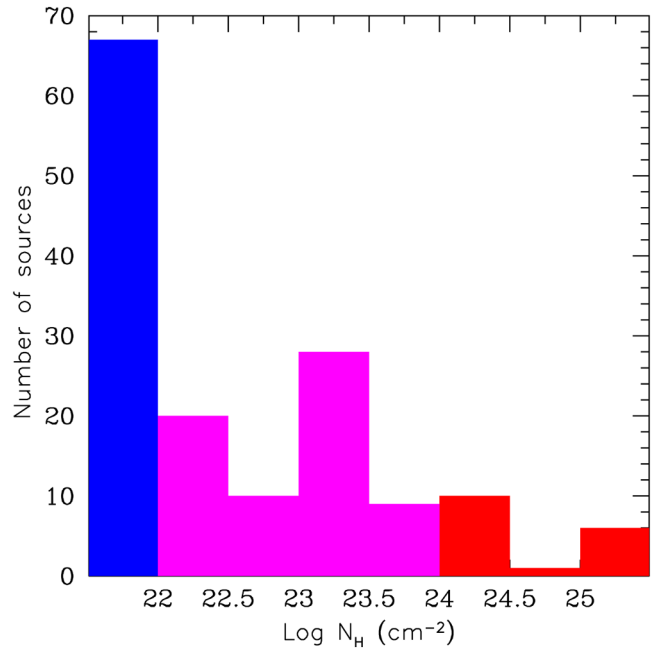

Fig. 7. Observed distribution of absorption columns. Unabsorbed ($N_H < 10^{22}$ cm^2), weakly absorbed ($10^{22} \leq N_H \leq 10^{24}$ cm^2) and Compton-thick ($N_H \geq 10^{24}$ cm^2) objects are shown in blue, magenta and red, respectively. From (Sazonov et al., 2015).

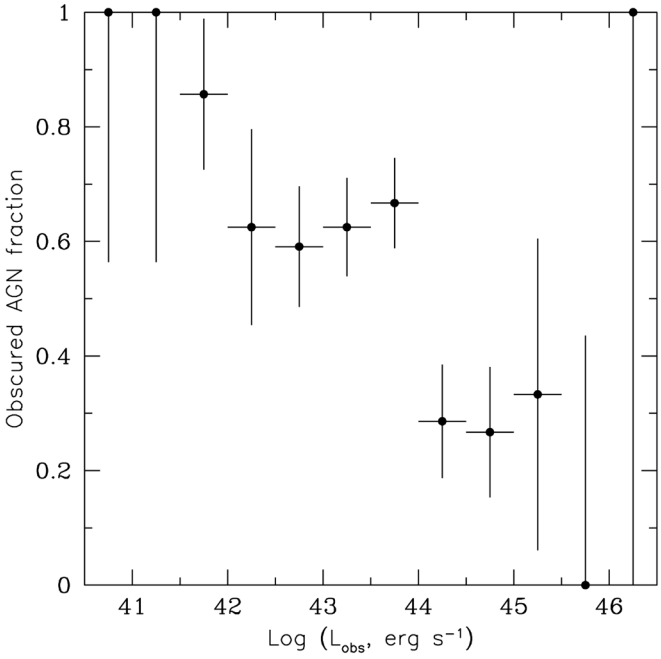

Fig. 8. Observed fraction of absorbed AGN as a function of observed hard X-ray luminosity. From (Sazonov et al., 2015).

Figure 8). A similar dependence has been independently established for the local AGN population using the *Swift*/BAT hard X-ray survey (Burlon et al., 2011) and for higher-redshift AGN with surveys conducted in the standard X-ray band (corresponding to the hard X-ray band in the rest-frame of quasars at $z \gtrsim 1$) (Ueda et al., 2014). Sazonov et al. (2015)suggested that this may be at least partially a selection effect, because not only hard X-ray, flux-limited surveys are negatively biased with respect to Compton-thick AGN, but hard X-ray selection is also positively biased with respect to unabsorbed ones (due to the reflection of part of the central source's hard X-ray radiation towards the observer). This implies that the intrinsic fraction of absorbed sources at a given luminosity must be higher than the observed one. Sazonov et al. (2015)further speculated that there is possibly no intrinsic declining trend of this fraction with luminosity if the hard X-ray emission from the accretion disc's corona is weakly collimated along its axis, as can well be the case. If so, the covering fractions of the torii in the local Seyfert galaxies should typically be as high as ~ 80–90%. Finally, Sazonov et al. (2015)demonstrated that Compton-thick objects intrinsically amount to nearly half of all absorbed AGN. Perhaps surprisingly, these hard X-ray findings are in good agreement with conclusions reached two decades ago based on optically selected samples of Seyfert galaxies (Maiolino and Rieke, 1995; Risaliti et al., 1999).

4.3. Luminosity Function

Together with *Swift*/BAT, *INTEGRAL*/IBIS multi-year observations have enabled an accurate determination of the hard X-ray luminosity function of local Seyfert galaxies. Apart from statistically characterising the supermassive black hole activity in present-day galactic nuclei, such a measurement is crucial for studying the cosmic history of black hole growth, since it provides an all-important $z = 0$reference point for the models of AGN evolution based on deep, pencil-beam X-ray surveys.

As already mentioned, shortly preceding the *INTEGRAL* measurements in the hard X-ray band, the AGN luminosity function was measured in the softer band of 3-20 keV in the XSS survey (Sazonov and Revnivtsev, 2004). This result was based on 95 local Seyfert galaxies and represented a substantial improvement over previous estimates obtained at energies below 10 keV thanks to the significantly reduced bias with respect to absorbed AGN and fairly large sample of objects. Nevertheless, XSS was still strongly biased against sources with $N_H > 10^{23}$ cm^{-2}and it was clear that yet harder (above 15 keV) large-area surveys were needed for a robust measurement of the luminosity function of local AGN.

The first AGN luminosity function based on *INTEGRAL* results was computed by Beckmann et al. (2006) in the 20–40 keV energy band using the aforementioned sample of 38 non-blazar AGN detected by IBIS over the first year of the mission. Most of the objects were nearby (the average redshift is 0.022). The derived luminosity function could be described by a broken power law, an empirical model commonly used in fitting AGN luminosity functions in various wavebands. Afterwards, Sazonov et al. (2007) made a more precise measurement of the hard X-ray luminosity function using a larger sample of IBIS-detected AGN (66 Seyfert galaxies).

The most recent version of the hard X-ray (17–60 keV) luminosity function of local AGN based on *INTEGRAL*/IBIS data is presented in Sazonov et al. (2015) (see Figure 9). As mentioned before, these authors used a sample of 151 Seyfert galaxies, which, compared to previous ones, covers broader ranges of distances and luminosities: $z \sim 0.001$–0.4 and $L \sim 3 \times 10^{40}$–2×10^{46} erg s^{-1}. It may nevertheless be considered a local one since most of the objects are located at $z < 0.1$. The derived luminosity function is in good agreement with that based on the *Swift*/BAT survey (Ajello et al., 2012). Apart from further tightening the parameters of the *observed*hard X-ray luminosity function, Sazonov et al. (2015)have also reconstructed the *intrinsic* luminosity function of local AGN by correcting for the observational biases related to X-ray absorption and reflection discussed in the preceding section. As a consequence, they determined the total intrinsic hard X-ray (17–60 keV) luminosity density of local AGN (with luminosities between $10^{40.5}$and $10^{46.5}$ erg s^{-1}): $\sim 1.8 \times 10^{39}$ erg s^{-1} Mpc^{-1}.

It is important to note that although there is substantial room for further improvement of local AGN statistics at the low end of the luminosity function (below $\sim 10^{41}$ erg s^{-1}), in particular with the eROSITA and ART-XC telescopes aboard the recently launched *Spektr-RG*satellite, there is no such possibility at the high end ($L \gtrsim 10^{45}$ erg s^{-1}) since *INTEGRAL*/IBIS and *Swift*/BAT have already

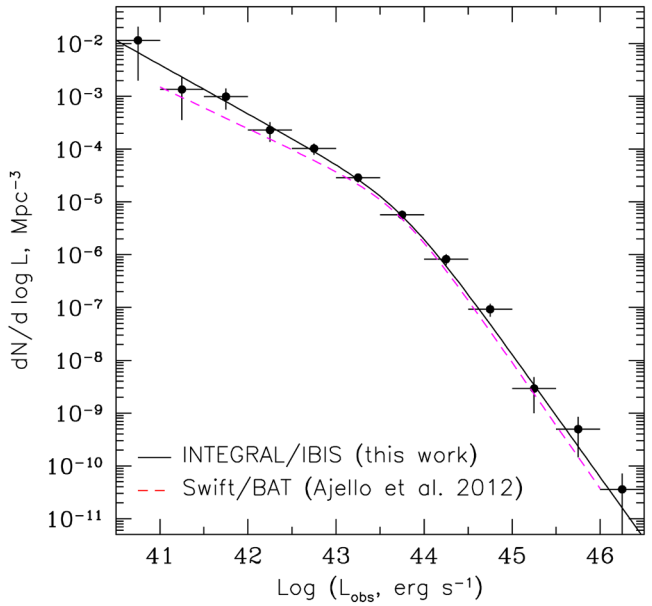

Fig. 9. Observed hard X-ray luminosity function of local AGN (circles) fitted by a broken power law (solid line). For comparison, the luminosity function based on the *Swift*/BAT survey (Ajello et al., 2012) is shown by the dashed line. From (Sazonov et al., 2015).

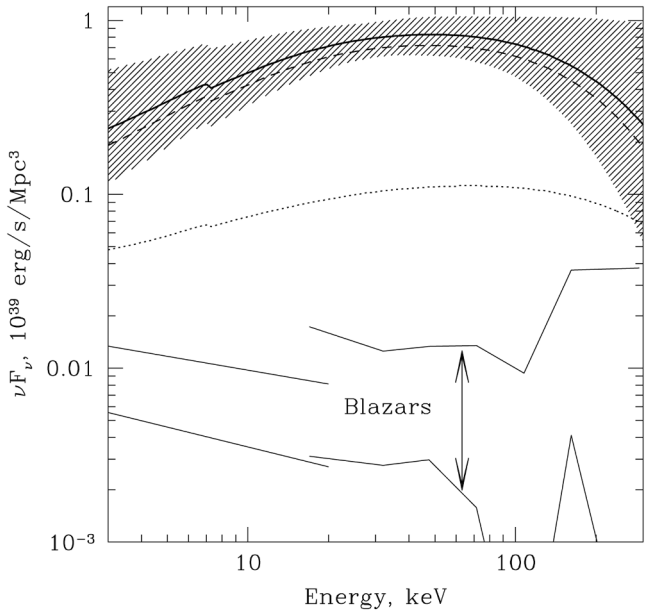

Fig. 11. Cumulative spectrum of the local Seyfert galaxies, based on *INTEGRAL* and *RXTE* data (solid line with the corresponding hatched uncertainty region) The dashed and dotted lines show the contributions of low- ($< 10^{43.5}$ erg s^{-1}) and high- ($> 10^{43.5}$ erg s^{-1}) luminosity AGN, respectively. The estimated contribution of blazars is also shown. From (Sazonov et al., 2008a).

probed the whole Universe out to $z \sim 0.2$at these luminosities and found just a few such quasar-like objects. This low number density of luminous AGN at the present epoch reflects the well-established fact that the main stage of growth of supermassive black holes took place in the remote past.

4.4. Links to the cosmic X-ray background

For a significant fraction of the extragalactic sky, in particular in the M81, LMC and 3C 273/Coma fields, IBIS observations have now reached a depth of ~ 0.2 mCrab. This has made it possible to measure the log N–log Sfunction of local Seyfert galaxies down to $\sim 3 \times 10^{-12}$ erg s^{-1} cm^{-2}(17–60 keV) (see Figure 4.4, Mereminskiy et al. (2016)). Although just ~ 2% of the CXB is resolved into point sources at these fluxes, the census of AGN conducted locally (at $z \lesssim 0.2$) by *INTEGRAL*and *Swift*is now nicely complemented by *NuSTAR* at higher redshifts ($z \lesssim 1$) (see Figure 4.4). Together with findings from deep extragalactic surveys performed in the standard X-ray band, these results have substantially tightened the constraints on the composition of the CXB.

In this context, an important result was presented by Sazonov et al. (2008a), who performed a stacking analysis of the X-ray spectra of AGN detected in the all-sky surveys performed by *INTEGRAL*/IBIS and *RXTE* (the aforementioned XSS survey), taking into account the space densities of AGN with different luminosities and absorbing column densities, i.e. the luminosity function and $N_H$distributions discussed above. They obtained the broad-band (3–300 keV) spectral energy distribution of the summed emission of the local AGN (see Figure 11). It exhibits (albeit with low significance) a cutoff at energies above 100–200 keV, in line with results obtained from broad band spectral studies of local AGN (see previous section (4.1)). It turned out that this locally determined spectrum is consistent with the CXB spectrum if the AGN population has experienced a pure

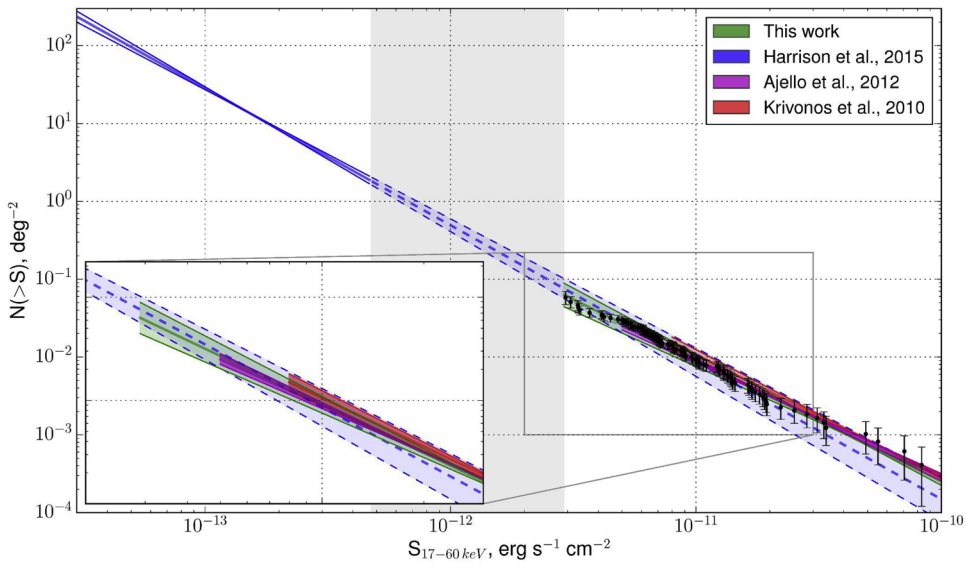

Fig. 10. AGN number-flux relations in hard X-rays measured by *NuSTAR* (Harrison et al., 2016), *Swift*/BAT (Ajello et al., 2012), in the *INTEGRAL*/IBIS all-sky survey (Maiolino and Rieke, 1995;) and in the *INTEGRAL*/IBIS deep fields (Mereminskiy et al., 2016). The shaded area demonstrates a flux region not yet probed by hard X-ray missions. The inset is a zoom of the range of the used data, see Mereminskiy et al. (2016).

luminosity evolution (so-called downsizing) between $z \sim 1$and $z = 0$,as is indeed indicated by the results of *Chandra*and *XMM-Newton* deep X-ray surveys (Barger et al., 2005). This nicely demonstrates that the popular concept of the CXB being a superposition of AGN is generally correct.

4.5. Spatial distribution

In the present-day Universe, matter is distributed very inhomogeneously on scales smaller than 100–200 Mpc. The contrast in matter density between large galaxy concentrations (superclusters) and voids can reach an order of magnitude and more. The vast majority of galaxies in the local Universe is believed to contain supermassive black holes in their nuclei. Most of them are currently dormant or only weakly active but a significant fraction ($\sim$ 1%) are accreting matter at high rates and manifest themselves as AGN (Seyfert galaxies). It is reasonable to expect the space density of AGN to be approximately proportional to that of normal galaxies. As the *INTEGRAL*all-sky hard X-ray survey provides a virtually unobscured view of the AGN population out to a few hundred Mpc, we have a unique opportunity to verify that AGN trace the cosmic large-scale structure.

Such a test has been done by Krivonos et al. (2007). They focused on the local volume of 70 Mpc radius, where maximal contrasts in galaxy counts are expected. Based on a subsample of $\sim$ 40Seyfert galaxies detected by IBIS, they demonstrated that AGN do follow closely the large-scale structure of the Universe, strongly concentrating in such well-known structures as the Virgo cluster, Great Attractor and Perseus-Pisces supercluster (see Figure 12). This result has subsequently been confirmed using the *Swift*/BAT survey (Ajello et al., 2012).

4.6. Bolometric properties

Hard X-ray observations primarily probe the emission produced in the hot corona of the accretion disc. Although this high-energy component constitutes a significant fraction of the bolometric luminosity of an accreting supermassive black hole, it is subdominant with respect to the softer (mainly UV) emission produced in the disc itself. A large fraction of the latter is in turn converted into even softer, infrared radiation in the surrounding dusty torus. In order to better understand the internal structure of AGN and physical processes taking place there, it is important to measure how the AGN bolometric luminosity is partitioned between these three main emission components (in radio galaxies and blazars, there may be an additional significant contribution from a relativistic jet, see below).

To this end, Sazonov et al. (2012) have utilised proprietary and archival data of *Spitzer* infrared observations for a sample of 68 local

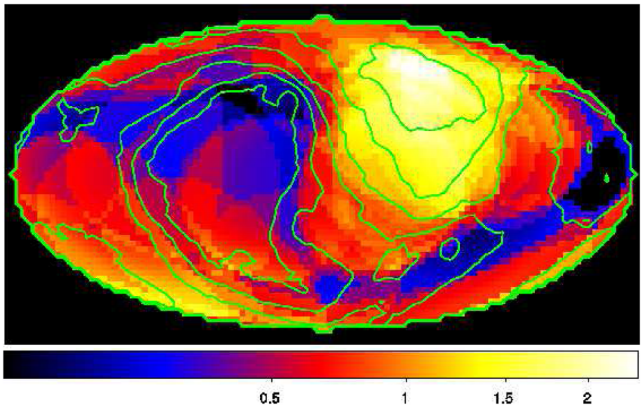

Fig. 12. 2D-map (in Galactic coordinates) of the AGN number density in the local Universe compared to that of normal galaxies. See (Krivonos et al., 2007) for details.

Seyfert galaxies detected by IBIS. They found a clear correlation between their hard X-ray and mid-infrared (MIR) luminosities: $L_{15\mu m} \propto L_{\rm HX}^{0.74\pm0.06}$,where $L_{15\mu m}$is the monochromatic luminosity at 15 μm and $L_{\rm HX}$is the luminosity in the 17–60 keV energy band. Assuming that the observed MIR emission is radiation from an accretion disc reprocessed in a torus that subtends a solid angle decreasing with increasing luminosity (as inferred from the declining fraction of absorbed AGN, see above), the authors inferred that the intrinsic disc luminosity, $L_{\rm disc}$,is approximately proportional to the luminosity of the corona, $L_{\rm corona}$,namely $L_{\rm disc}/L_{\rm corona} \sim 2$. This ratio is a factor of $\sim$ 2smaller than inferred for typical (more distant and luminous) quasars producing the CXB (Sazonov et al., 2004a). The authors further demonstrated that the hard X-ray (17–60 keV) luminosity is a good proxy of the bolometric luminosity, $L_{\rm bol}$,of Seyfert galaxies, with a typical ratio $L_{\rm bol}/L_{\rm HX} \sim 9$. This, together with black hole mass estimates available for the same sample of AGN, was used by Khorunzhev et al. (2012)to infer the Eddington ratios of these objects, which turned out to lie between 1 and 100% for the majority of them. Finally, Sazonov et al. (2012)estimated the cumulative bolometric luminosity density of local AGN, which turns out to be $\sim 2 \times 10^{40}$ erg s^{-1} Mpc^{-3}.

5. Main Results: Radio Galaxies

Radio galaxies are sources showing on radio maps an extended structure with lobes and jets. Historically, they have been divided into two classes on the basis of their radio morphology: FRI, having bright jets in the centre and low total luminosity and FRII, having faint jets but bright hot spots at the ends of the lobes and high total luminosities (Fanaroff and Riley, 1974). The different morphology probably reflects the method of energy transport in the radio source: FRIIs appear to be able to transport energy efficiently to the ends of the lobes, while FRI beams are inefficient in the sense that they radiate a significant amount of their energy away as they travel. The cause of the FRI/FRII difference is still unknown and both external properties (environment, host galaxy, merging history, etc.) or intrinsic factors (different accretion processes) have been used to explain this dichotomy without reaching up to now firm conclusions.

A further subdivision among radio galaxies has recently come from their optical spectroscopic properties (Buttiglione et al., 2010): in general, objects with and without high-excitation emission lines in their optical spectra are referred to as High Excitation Radio Galaxies (HERG) and Low Excitation Radio Galaxies (LERG) respectively. HEG accrete in a radiatively efficient manner due to high Eddington ratios ($\geq$0.01 and up to 1) while LEG are known to exhibit radiatively inefficient accretion related to low Eddington ratios ($\leq$0.01).

The jets of radio galaxies are oriented at inclination angles typically greater than 10 degrees with respect to the line of sight, making these objects intermediate between radio loud blazars and classical radio quiet Seyferts: it is for this reason that radio galaxies are unique laboratories where to study at the same time jets and accretion processes and search for a connection between the two.

A recent investigation done by Bassani et al. (2016) show that radio galaxies are not common among hard X-ray selected AGN: for example within the sample of around 400 AGN detected by *INTEGRAL*/IBIS up to 2016, (Malizia et al., 2016) only 32 (i.e. 8%of the sample) are radio galaxies. These *INTEGRAL*selected radio galaxies cover all optical classes, are characterised by high 20-100 keV luminosities (10^{42}–10^{46}erg s^{-1}) and high Eddington ratios (typically larger than 0.01). Most of these objects display a FRII radio morphology and are classified as HERG. Several studies have been performed on *INTEGRAL*high energy selected sample of radio galaxies in order to investigate their spectral characteristics.

Panessa et al. (2016) studied the absorption properties of this sample with the addition of radio galaxies detected by *Swift*/BAT and found that the column density distribution is consistent with the unified

model of AGN with those optically classified as type 2 being absorbed and those optically classified as type 1 not. However, there seems to be no evidence for the presence of Compton thick absorption in hard X-ray selected radio galaxies (Ursini et al., 2018a). Also a significant anti-correlation between the radio core dominance parameter (taken as an orientation indicator) and the X-ray column density is found, again in line with expectations from the AGN unified theory: core dominated sources are unabsorbed in X-rays since they emit their radiation in a direction closer to the line of sight and therefore not intercepted by the torus.

The broad band spectra of some *INTEGRAL* detected radio galaxies have been studied over the years by various authors (Beckmann et al., 2011; Malizia et al., 2014; Molina et al., 2014; Lubiński et al., 2016; Molina et al., 2015; Ursini et al., 2018b) and the overall result is that they behave very similarly to radio quiet AGN in terms of primary continuum, presence of complex absorption and soft excess, with the possible exception of the reflection features (10–30 keV bump and iron line) which tend to be weak in these objects.

These observational results confirm that the high energy properties of these sources are consistent with an accretion-related emission, likely originating from a hot corona coupled with a radiatively efficient accretion flow.

The radio size distribution of the entire *INTEGRAL* sample of radio galaxies shows an almost continuous coverage, from around 50 kpc (in PKS 0521-365) up to 1.5 Mpc (in IGR J14488-4008), with many sources displaying values above few hundred kpc; indeed 56%of the objects in the sample have sizes above 0.4 Mpc. If we consider the classical threshold to define a giant radio galaxy (GRG), i.e. a size larger than 0.7 Mpc, then in the *INTEGRAL*sample of 32 radio galaxies, 8 are giants, i.e. 25% of the sample. It may be the case that high-energy surveys could be more efficient in searching for new GRG as compared to radio surveys, where, for example, in the well studied 3CRR sample, only 6%of the sources are identified as GRG (Bassani et al., 2016). That a large fraction of hard X-ray selected radio sources become radio giants is also evident by the discovery of two completely new GRG among *INTEGRAL*AGN: IGR J17488-2338 (Molina et al., 2014) and IGR J14488-4008 (Molina et al., 2015), which display peculiar and interesting radio as well as soft and hard X-ray properties. In Figure 13 the radio 610MHz GMRT full resolution image of IGR J14488-4008 as published by Molina et al. (2015) is displayed: evident from the figure are the large size of the source, its FRII morphology and also its interesting environment.

All 8 *INTEGRAL* selected GRG have been the focus of an intense observational campaign especially at radio frequencies to probe the possibility of restarting activity in their nuclei. In fact in these giants, the luminosity of the radio lobes and the estimated jet power are relatively low compared with the nuclear X-ray emission (Ursini et al., 2018b). This indicates that either the nucleus is more powerful now than was in the past, consistent with a restarting of the central engine, or that the giant lobes are dimmer due to expansion losses. The first scenario is backed up by the finding in the radio band that 6 objects (75%of the sample) host a core with a self absorbed spectrum (peaking in the range from 2 to 10 GHz or above) typical of young radio sources (ages of kyears) while their extended structure must be very old and evolved (ages of Myears): these young nuclei are probably undergoing a restarting activity episode, suggesting a link between the detected hard X-ray emission, due to the ongoing accretion, and the reactivation of their jets (Bruni et al., 2019). Of the two sources not showing a young radio core spectrum, one has the radio lobes embedded in an extended low surface brightness cocoon, that is likely the result of a previous period of activity (Weżgowiec et al., 2016). The other source presents instead a discontinuity between the extended lobes and the arcsec core-jet structure again pointing towards the presence of different activity phases (Giovannini et al., 2007). These findings support the scenario originally proposed by Subrahmanyan et al. (1996), in which multiple episodes of activity would favour the growth of radio sources up to the extreme size of GRGs but also underline the importance of extracting hard X-ray selected samples of radio galaxies with the purpose of studying the duty cycle of AGN.

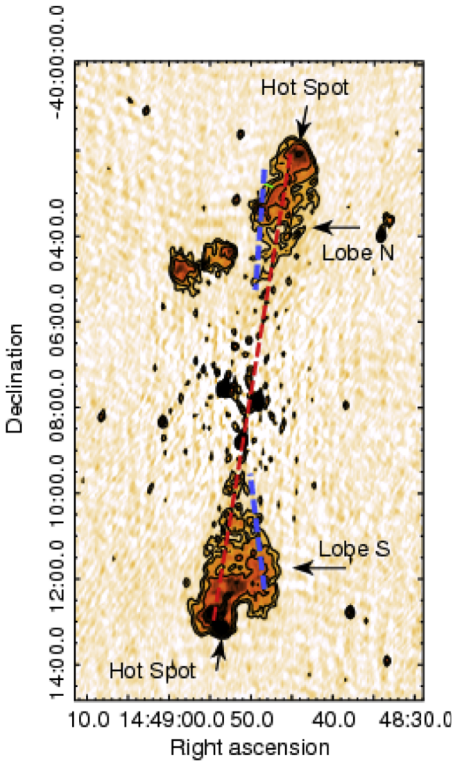

Fig. 13. Radio 610MHz GMRT full resolution image of IGR J14488-4008 as in Molina et al. (2015)

6. Main Results: Blazars

Among radio-loud AGN, blazars are the most luminous and variable. This is because strong relativistic aberration effects, primarily light magnification and time intervals foreshortening, take place in the plasma flowing at speeds close to that of light in their powerful jets, that are oriented only a few degrees away from the line of sight. They include both flat-spectrum radio quasars (FSRQ) and BL Lacertae objects (BL Lac). BL Lacs are further classified into low/intermediate/high-frequency-peaked BL Lac objects (LBL, IBL, HBL) depending on the location of the first characteristic peak frequency: below 10^{14}Hz, at 10^{14-15}Hz, or above 10^{15}Hz, respectively. Both blazar classes share the properties of a nonthermal continuum, but FSRQ have strong and broad optical emission lines, while in BL Lac the optical lines are weak or absent. FSRQ have higher bolometric luminosities than BL Lac (Sambruna et al., 1996) and can exhibit signs of thermal activity possibly related to an accretion disc in their optical and UV spectra (Smith et al., 1988) in contrast to BL Lac, which have smooth continua.

Multiwavelength studies of blazars in the last 25 years have identified a characteristic broad-band spectral shape, with two ”humps” in a νf_νrepresentation (Falomo et al., 2014). The first hump, peaking at mm to soft X-ray frequencies (depending on the source, and varying even in the same source during different emission states), is produced by synchrotron radiation, while the origin of the second hump, that has a maximum between MeV and GeV energies, is complex, with various scenarios contemplating a pure leptonic composition of the jet or a lepto-hadronic composition. In the leptonic case, the high energy hump can be due to inverse Compton scattering of relativistic electrons or positrons off synchrotron photons (internal Compton or self-Compton) or off ambient photon fields, if these are relevant, as in the case of FSRQ that, as said before, host luminous accretion discs and broad emission

lines (external Compton). For the lepto-hadronic scenario, if sufficient energy is injected in the jet to trigger photo-pion production, synchrotron-supported pair cascades will develop (Boettcher (2010); Murase (2017)and references therein). These initiate showers of mesons, leptons, neutrinos and high energy radiation.

According to the location of the two radiation peaks, blazars form a "sequence" (Fossati et al., 1998; Ghisellini et al., 1998) whereby sources with peaks at lower frequencies have larger luminosities and larger ratios between the high-energy and low-energy components (see however Padovani et al. (2012)). The blazars with largest bolometric luminosities, largest dominance of gamma-ray luminosities, lowest frequencies of the synchrotron and highest energy Compton hump, generally coincide with the FSRQ, in whose jets relativistic particles cool rapidly by losing energy in Compton upscattering disc and line optical-UV photons. The less-efficiently cooling, less luminous sources coincide with the BL Lac objects.

Blazars represent almost 70% of all sources detected at energies larger than 100 MeV by the *Fermi*/LAT instrument (The Fermi-LAT collaboration, 2019). This, together with the fact that most blazars are bright X-ray sources, makes them also excellent targets for hard X-rays studies. Indeed various *INTEGRAL* surveys list a conspicuous number of them.

For example considering all the AGN detected by *INTEGRAL* (see Malizia et al. (2012); Malizia et al. (2016) and more recent updates), we count 29 FSRQ and 19 BL Lac, around 11% of the entire *INTEGRAL* AGN population (see Figure 4). Interestingly all 8 blazars listed in the complete sample of AGN discussed by Malizia et al. (2009) have now a counterpart at GeV energies, with 3 also having a TeV association: this indicates that these are bright enough for detection up to the highest observable energies.

Blazars detected by *INTEGRAL* have been used over the years to provide information on their high-energy variability patterns (Beckmann et al., 2007), to monitor individual targets over a period of intense activity (see for example Figure 14 which shows the light curves of MKN 421 during a flare recorded in April 2013 by Pian et al. (2014)), or to study their broad band spectral characteristics such as in the case of 4C 04.42, where excess emission observed in the soft X-ray band was interpreted as due to bulk Compton radiation of cold electrons (de Rosa et al., 2008).

According to the locations of the two spectral peaks in blazar energy distributions, the hard X-ray region represents either the tail of the synchrotron spectrum at energies higher than the cooling break, or the rising portion of the inverse Compton (leptonic case) or proton-synchrotron (lepto-hadronic case) spectrum. HBL, and in particular those peaking in X/hard X-rays, are prominent in the 20-200 keV band, and having the lowest jet powers, represent the extreme end of the blazar sequence, opposite to FSRQ. One such example of extreme blazar was discovered by *INTEGRAL* in the source IGR J19443+2117 (Landi et al., 2009) which was later detected also by the Cherenkov telescope *HESS* as HESS J1943+213 (H. E. S. S. Collaboration et al., 2011; Archer et al., 2018): the source displays a synchrotron peak at around 10 keV and an inverse Compton peak above few hundred of GeV.

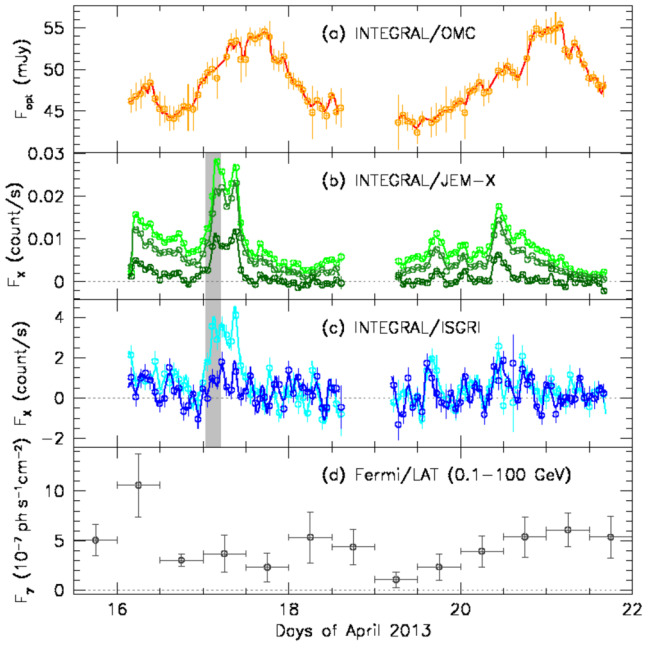

Fig. 14. Light curve of MKN 421 in April 2013, see Pian et al. (2014)

During bright outbursts of "extreme" HBL, the synchrotron spectrum, normally peaking at soft X-rays, flattens and reaches a peak at energies equal or higher than 100 keV, as observed first in the BL Lac object MKN 501 in 1997 with *BeppoSAX* (Pian et al., 1998). Thus, depending on whether the blazar has a high-frequency or low-frequency synchrotron peak, IBIS observations will sample the rising part of the inverse Compton component or the tail of the synchrotron, thus allowing one to locate more precisely the peaks of these radiation components and to extract precise information on the energies of the emitting particles (Bottacini et al., 2016).

Equally important for hard X-ray studies are FSRQ located at high redshifts displaying a Compton peak in the sub-MeV region which also favour their detection by instruments like *INTEGRAL*/IBIS. These sources have the most powerful jets, the largest black hole masses and the most luminous accretion discs. *INTEGRAL* has played a role in the discovery of such high redshift blazars like IGR J22517+2217 (Bassani et al., 2007; Lanzuisi et al., 2012), Swift J1656.3-3302 (Masetti et al., 2008a) and IGR J12319-0749 (Bassani et al., 2012). So far 17 objects have been detected at redshift greater than 1, with 3 having $z$above 3. The most distant AGN so far detected by *INTEGRAL*, the FSRQ IGR J22517+2217, has been the target of intense studies after the *INTEGRAL*detection (Lanzuisi et al., 2012) which lead to various results: the discovery of a strong flare episode, the study of the source SED over flaring and quiescent states (see Figure 15) and the measurement of a flare jet power luminosity which turned out to be around 30 times more powerful than the accretion disc luminosity.

INTEGRAL/IBIS's sensitivity of ~10 mCrab in the 20-100 keV range implies that most blazars can be detected with a high statistical significance only when they are in a high emission state. Therefore, they are generally observed with *INTEGRAL*during outbursts, after a notification from a large field of view X-ray or gamma-ray camera, like e.g. *Swift*/BAT, *MAXI, Fermi*/LAT, or *AGILE*/GRID. This "Target-of-Opportunity" strategy is rather effective, but implies that *INTEGRAL*can typically cover the declining phase of the outburst, owing to the characteristic ~1-2 days re-pointing time of the satellite. The simultaneous monitoring of *INTEGRAL*, primarily with IBIS, but in some cases also with the JEM-X cameras (3-30 keV), and other multiwavelength facilities have set cogent constraints on the physics that governs blazar correlated flux and spectral variability over the whole electromagnetic spectrum (e.g. Pian et al. (2006); Ghisellini et al. (2007); Vercellone et al. (2011); Collmar et al. (2010); Pian et al. (2011); Castignani et al. (2017)).

Owing to their luminosities, blazars are, after gamma-ray bursts, the farthest detectable sources at all wavelengths and therefore potential beacons of the early Universe. The cosmological relevance of blazars was not missed by the *INTEGRAL* mission, that enabled not only the detection of previously unknown ones at high redshift but also the monitoring of a few previously known distant ones as in Pian et al. (2005); Bianchin et al. (2009); Bottacini et al. (2010a); Gianní et al. (2011).

The *IceCUBE* detection of a ~200 TeV neutrino from blazar TXS0506+056 (z= 0.336) on 22 September 2017 confirmed many expectations that powerful extragalactic jetted sources may be the origin of high-energy (i.e. E > 1TeV) neutrinos. This detection also

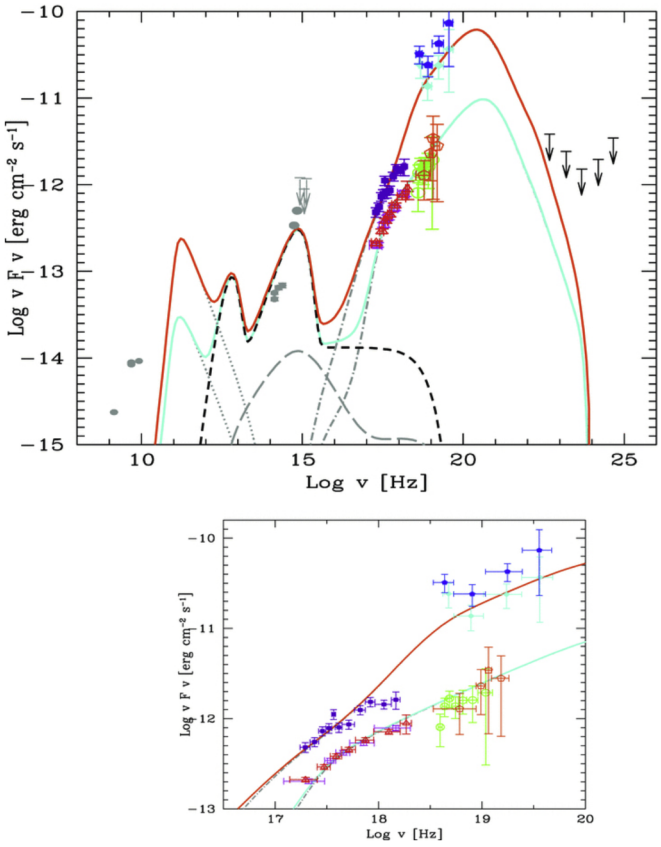

Fig. 15. Top: spectral energy distribution of IGR J22517 + 2217. Grey circles and arrows represent archival radio/optical/UV data from NED. Red triangles and magenta squares represent XIS 0 and XIS 3 data, green circles and orange pentagons represent PIN and BAT quiescent data respectively, while black arrows are Fermi upper limits in five bands. Filled violet squares represent XRT data, filled cyan diamonds and blue pentagons represent IBIS and BAT flare data respectively. The solid cyan and orange curves are the results of modelling of the quiescent and flaring states, respectively. With grey lines we show the different components of non-thermal emission: synchrotron (dotted), synchrotron self-Compton (long-dashed) and external Compton (dot dashed). The black dashed line corresponds to the thermal emission of the disc, the IR torus and the X-ray disc corona. The model does not account for radio emission, produced from much larger regions of the jet. Bottom: enlargement in the X-ray energy range for the two SEDs. Symbols as in the top panel. Figure from Lanzuisi et al. (2012)

unambiguously points to the presence of a hadronic component in the jet composition, as only hadronic showers can induce cascades that include neutrinos as by-products. A multiwavelength observing campaign was launched as a consequence of the detection, that included *INTEGRAL* among the many space-based facilities that were employed (IceCube Collaboration et al., 2018). The resulting spectra and light curves and their correlations, combined with the neutrino event, were used to test blazar lepto-hadronic models, in an attempt to determine the mutual role of leptons and hadrons in producing radiation (Keivani et al., 2018; Gao et al., 2019; Righi et al., 2019). While neutrino events accompanying blazars are rarely detected with the present instrumentation, they represent a formidable diagnostic of the structure and mechanisms in relativistic jets.

7. keV to GeV/TeV connection: a case study

The connection between the hard X-ray region of the spectrum and the GeV/TeV domain is critical for the study of many AGN, blazars *in primis* (see previous section), but also for radio galaxies and Seyferts galaxies. In these last two types of objects, it is important to understand how to connect the emission due to the disc/corona which dominates at lower energies, to the one related to the jet or some other mechanism (starburst?) which instead dominate at higher frequencies.

Ubertini et al. (2009) presented for the first time the result of the cross correlation between the fourth *INTEGRAL*/IBIS soft gamma-ray catalogue and the *Fermi*/LAT bright source list of objects emitting in the 100 MeV–100 GeV range. Surprisingly, from this initial cross-correlation between low and high energy gamma-ray sources emerged that only an handful of objects were common to both surveys; they comprised blazars (10) both of FSRQ and BL Lac types, and no X-Ray Binaries, with the only exception of two microquasars.

This initial approach can now be applied further by finding objects, among *INTEGRAL* detected AGN, that emit also at GeV and/or at TeV energies.

This can be done by cross-correlating our list of 440 AGN with the most recent *Fermi*/LAT catalogue[2] and the TeV on line catalogue[3]. From this cross correlation, interesting results have been found and reported here to highlight *INTEGRAL*'s capability in this field. The standard statistical technique developed by Stephen et al. (2005) has been used. It consists of simply calculating the number of GeV/TeV sources for which at least one INTEGRAL counterpart was found within a specified distance, out to a distance where all GeV/TeV sources had at least one soft-gamma ray counterpart. To have a control group, a list of 'anti GeV/TeV sources', mirrored in Galactic longitude and latitude, has been created and the same correlation algorithm applied. In both cases a correlation out to about 300 arcsec has been found, while at further distances, chance correlations become increasingly more important. At GeV energies 58 *INTEGRAL* AGN (13%of the sample) have emission above 1 GeV, while only 15 objects (3%of the sample) emit up to TeV energies, confirming that the emission of the majority of hard X-ray selected AGN drops exponentially above 100-200 keV. The GeV sample is largely dominated by blazars: there are 18 BL Lac and 24 FSRQ. Other sources include 9 radio galaxies, 3 Seyfert 2 (NGC 1068, NGC 4945 and the Circinus galaxy), one NLS1 galaxy (1H 0323 + 342), one peculiar object (IGR J20569 + 4940) and two sources of unclear class (IGR J18249-3243 and IGR J13109-5552). Two radio galaxies detected in the GeV band are also TeV emitters, while none of the 4 Seyfert galaxies have so far being detected at TeV energies. Interestingly of the 18 BL Lac objects detected by *Fermi*/LAT, 11 have been seen also by Cherenkov telescopes: they are mostly high frequency peaked objects, 8 HBL and 2 IBL. Their Compton peak is generally just below 1 TeV but can be as high as 10 TeV or more like in H 1426 + 428 (Foffano et al., 2019).

A peculiar source is IGR J20569 + 4940. It is certainly a blazar but still of unknown class and redshift: the source has recently been announced as a VHE emitter (Benbow and VERITAS Collaboration, 2017) after observations with *VERITAS* performed in November 2016. It is most likely a BL Lac (Chiaro et al., 2016) with a high synchrotron peak (Fan et al., 2016). In Figure 16, we assembled high energy data on this source using an unpublished *NuSTAR* observation performed in November 2015 with the average *INTEGRAL* and *Fermi*/LAT spectra plus the reported TeV data. As evident from the figure, two peaks can be located, one below the *NuSTAR* low energy threshold, at around few keV, likely associated to the synchrotron part of the SED, and the other at around 0.1-0.3 TeV, probably related to the Compton part of the SED. This qualifies IGR J20569 + 4940 to be another HBL or alternatively another extreme BL Lac.

As for the FSRQ, the set of *INTEGRAL* objects with GeV emission spans a wide range of redshifts (0.3-3.1) and black hole masses (Log ($M/M_{\odot}$) = 8-9.5). As discussed in the previous section, these sources display the most powerful jets, they are very massive, host the largest

[2] 8 year point source catalogue: https://heasarc.gsfc.nasa.gov/W3Browse/fermi/fermilpsc.html

[3] http://tevcat.uchicago.edu

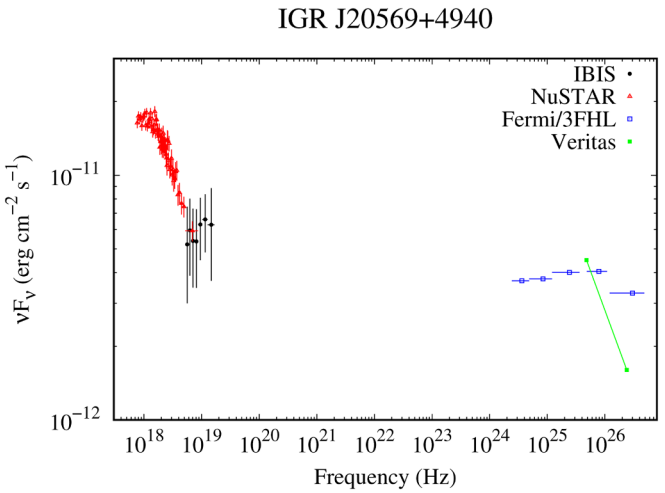

Fig. 16. Spectral Energy Distribution of IGR J20569 + 4940 obtained assembling unpublished *NuSTAR* observation performed in November 2015 with the average *INTEGRAL* and *Fermi*/LAT spectra with the addition of the reported TeV data (courtesy of F. Ursini).

black hole masses and the most luminous accretion discs; in other words they are more extreme than blazars selected in other wavebands, like, for example, the only one explored by *Fermi*/LAT (Bassani et al., 2013).

Only 4 of the 24 GeV FSRQ in our list have a detection at TeV energies, namely 3C 279, PKS 1510-089, PG 1222 + 216 and SWIFT J0218 + 7348. This low number of detections is expected since FSRQ are generally faint at very high energies for a number of reasons: the location of their Compton peak at the lower end of the high energy gamma ray band implies a low flux at these energies; the compactness of the source emission region indicates strong attenuation by the broad line region photon field and, finally, their rather high redshifts (H. E. S. S. Collaboration et al., 2019).

However, the same reasons indicate that it is important to study the SED of these peculiar FSRQ and soft gamma ray observations can be of great help to better define their spectral energy distribution.

Among *INTEGRAL* AGN with GeV emission, there are a couple of sources of unclear class: IGR J18249-3243 and IGR J13109-5552. Optically they are both classified as Seyfert 1. They are both bright in the radio waveband and, although repeatedly observed, are poorly studied. Their structure seems to be extended but a dedicated observational campaign is necessary to confirm the presence of jet and related features. The broad band (*XMM* plus IBIS/BAT data) properties of both objects have been explored by Malizia et al. (2014). Unlike other Seyfert galaxies and similarly to what we observe in blazars neither source shows a low energy cut-off (≥357 keV in IGR J13109-552 and not required in IGR J18249-3243). Furthermore, in IGR J18249-3243 partial covering absorption is present, like in an ordinary radio quiet Seyfert, making the picture even more confused. Clearly both sources deserve further investigation, possibly through a multiwaveband campaign that will be able to clarify their nature.

7.1. TeV blazars

Nearly all identified extragalactic TeV emitters are blazars (about 70 sources), exceptions being a handful of nearby radio galaxies and starburst galaxies and a recently detected long gamma-ray burst at $z = 0.4$. The brightest blazars in the TeV domain are the HBL, i.e. those whose high energy component peaks in or just beyond that band. These sources are ideal targets of coordinated hard X-ray and TeV observing campaigns (e.g. Ahnen et al. (2016, 2018); Chevalier et al. (2019)and references therein).

Prototype blazars with these characteristic spectral energy distributions are MKN 421 and MKN 501, that are also the brightest objects of this class. They may reach "extreme" states whereby the synchortron spectrum extends to energies higher than 100 keV during flares and the TeV emission increases by more than one order of magnitude with respect to the quiescent state. Recent simultaneous monitoring at hard X-rays and TeV energies with *NuSTAR* and the *Veritas* Cherenkov telescope respectively, combined with observations at optical and radio frequencies, yielded detailed insight into the physics of these sources, with accurate mapping of critical parameters such as electron energies and Lorentz factor (Furniss et al., 2015; Sinha et al., 2015; Baloković et al., 2016). Repeated observations of HBLs in bright states, as triggered by *Swift*/XRT or atmospheric Cherenkov radiation telescopes, and in particular of the nearby BL Lac object MKN 421 with *INTEGRAL*, sampled bright states and collected detailed light curves and spectra (Lichti et al., 2008; Pian et al., 2014). The type of X-ray variability suggests a complex behaviour and a correlation among different frequencies. However, so far, although IBIS detected rather hard spectra, no clear evidence was found that these still rise (in νf_ν) beyond 15-20 keV. Investigation with IBIS of the BL Lac object MKN 501, in search of a shift of the synchrotron peak to hard X-rays during outbursts in 2013 and 2014 is underway.

A few dimmer BL Lac share the "extreme" properties of MKN 421 and MKN 501 and are potential ideal targets for coordinated hard X-ray and TeV monitoring (Costamante et al., 2018). In the near future, these can be followed-up with the sensitive Cherenkov Telescope Array for more accurate assessment of their physical parameters than it is possible with present state-of-the-art Cherenkov telescopes.

Particularly interesting are the so called "orphan" gamma-ray flares, whereby some sources exhibit strong TeV outbursts that are not accompanied by simultaneous X-ray flux increase at any appreciable level (e.g. Krawczynski et al. (2004); Bottacini et al. (2010b); MacDonald and Mullan (2017)).

8. INTEGRAL heritage and future perspectives

INTEGRAL's cumulative exposure has now exceeded 10 Ms in several extragalactic fields with a total area of ∼ 2000sq. deg. and IBIS has detected ∼ 100AGN (known or presumed) with fluxes down to 3×10^{-12} erg s^{-1} cm^{-2}(17–60 keV) in these regions. This sample is a valuable part of the *INTEGRAL*– *Swift* legacy, since it widens the AGN parameter space to lower luminosities and larger distances. In particular, a significant fraction of AGN detected at these (low) fluxes are expected to be located at $z \simeq 0.2$,which makes it possible to begin studying the evolution of the AGN population over the last ∼ 2.5billion years in a nearly unbiased way (thanks to the hard X-ray selection). To this end, it is highly desirable to further lower the flux threshold in the INTEGRAL extragalactic fields, which can be done by adding exposure since the IBIS sensitivity is still largely determined by statistical noise in the extragalactic sky.

Activities in this direction are already under way. In particular, in 2017–2018 there were extensive observations of the ultra-deep field in the Virgo region (PI: Beckmann) and in 2019–2020 the deep field around the M81 galaxy is to be observed for an additional 3.75 Ms (PI: Mereminskiy), which will bring the total exposure there to ∼ 15Ms and the corresponding flux limit to $\sim 2 \times 10^{-12}$ erg s^{-1} cm^{-2}(17–60 keV). Some 50 new AGN are expected to be detected upon completion of this programme (and there are suggestions to continue it afterwards). Moreover, there is expected to be unique synergy between these *INTEGRAL*observations and the upcoming all-sky X-ray survey by the *Spektr-RG* observatory (with its eROSITA and ART-XC telescopes). The latter is expected to reach record sensitivities $\sim 10^{-14}$,$\sim 2 \sim 10^{-13}$and ∼a few 10^{-13}erg s^{-1} cm^{-2}in the 0.5–2, 2–10 and 5–11 keV energy bands, respectively, after 4 years of observations, while shallower maps will be available already after the first 6-month scan of the sky. *INTEGRAL*hard X-ray observations and *Spektr-RG* data at lower energies in the M81 field will be complementary in a number of ways, in particular

regarding the detection and identification of Compton thick AGN.

It is worth noting that, although deep surveys on specific sky regions are important to probe lower luminosity objects and further distance scales, it is only through large scale mapping that is possible to enlarge the *INTEGRAL* AGN database. By extrapolating from previous surveys, it is also possible to estimate how many AGN *INTEGRAL* will be able to detect in the future. From the sky coverage obtained in 2000 orbits (September 2018), we expect to double the number of the detected AGN and we foresee that we will be able to observe more than 1200 AGN by revolution 2500, likely by the end of the mission. Even more interesting is the ongoing monitoring of the Galactic Plane region by *INTEGRAL*. As already mentioned, this is a region which is generally avoided by extragalactic studies and where *INTEGRAL* is playing an even greater role than *Swift*/BAT. In this region, deep sky coverage combined with large scale mapping, will allow a unique view of the extragalactic sky behind our Milky Way across the years, a legacy which will be extremely useful for future studies of this region at other wavelengths, especially for the *Cherenkov Telescope Array* (CTA) future surveys.

On the other hand, the advent of the *CTA* in the near future and the sensitivity upgrades of neutrino detectors will result in a boost of multiwavelength and multi-messenger studies of high energy extragalactic sources, and help unveil the physics of their complex central engines.

List of abbreviations

List of definitions of abbreviations used in the paper.
NLS1: Narrow Line Seyfert 1
XBONG: X-ray Bright Optically Normal Galaxies
LINERs: Low-Ionization Nuclear Emission Regions
FSRQ: Flat Spectrum Radio Quasar
BL Lac: BL Lacertae
LBL, IBL, HBL: low/intermediate/high-frequency-peaked BL Lac objects
RG: Radio Galaxies
FRI: Fanaroff type I
FRII: Fanaroff type II
HERG: High Excitation Radio Galaxies
LERG: Low Excitation Radio Galaxies
GRG: Giant Radio Galaxies

Declaration of Competing Interest

None.

Acknowledgements

We acknowledge all the scientists which contributed over the years to the analysis and the interpretation of INTEGRAL AGN data. In particular we would like to thank Nicola Masetti for his fundamental work in leading the optical follow-up campaigns of the unidentified INTEGRAL sources. We thank also J. B. Stephen for his contribution in the correlation studies presented in this work. AM and LB acknowledge financial support from ASI under contract INTEGRAL ASI/INAF n.2019-35-HH; SS and IM acknowledge support from the Russian Science Foundations grant 19-12-00396 in working on this review.

References

Ahnen, M.L., Ansoldi, S., Antonelli, L.A., Antoranz, P., Babic, A., Banerjee, B., Bangale, P., Barres de Almeida, U., Barrio, J.A., Becerra González, J., Bednarek, W., Bernardini, E., Biasuzzi, B., Biland, A., Blanch, O., Bonnefoy, S., Bonnoli, G., Borracci, F., Bretz, T., Buson, S., Carosi, A., Chatterjee, A., Clavero, R., Colin, P., Colombo, E., Contreras, J.L., Cortina, J., Covino, S., Da Vela, P., Dazzi, F., De Angelis, A., De Lotto, B., de Oña Wilhelmi, E., Di Pierro, F., Domínguez, A., Dominis Prester, D., Dorner, D., Doro, M., Einecke, S., Eisenacher Glawion, D., Elsaesser, D., Fernández-Barral, A., Fidalgo, D., Fonseca, M.V., Font, L., Frantzen, K., Fruck, C., Galindo, D., García López, R.J., Garczarczyk, M., Garrido Terrats, D., Gaug, M., Giammaria, P., Godinović, N., González Muñoz, A., Gora, D., Guberman, D., Hadasch, D., Hahn, A., Hanabata, Y., Hayashida, M., Herrera, J., Hose, J., Hrupec, D., Hughes, G., Idec, W., Kodani, K., Konno, Y., Kubo, H., Kushida, J., La Barbera, A., Lelas, D., Lindfors, E., Lombardi, S., Longo, F., López, M., López-Coto, R., Majumdar, P., Makariev, M., Mallot, K., Maneva, G., Manganaro, M., Mannheim, K., Maraschi, L., Marcote, B., Mariotti, M., Martínez, M., Mazin, D., Menzel, U., Mirand a, J.M., Mirzoyan, R., Moralejo, A., Moretti, E., Nakajima, D., Neustroev, V., Niedzwiecki, A., Nievas Rosillo, M., Nilsson, K., Nishijima, K., Noda, K., Nogués, L., Orito, R., Overkemping, A., Paiano, S., Palacio, J., Palatiello, M., Paneque, D., Paoletti, R., Paredes, J.M., Paredes-Fortuny, X., Pedaletti, G., Perri, L., Persic, M., Poutanen, J., Prada Moroni, P.G., Prandini, E., Puljak, I., Rhode, W., Ribó, M., Rico, J., Rodriguez Garcia, J., Saito, T., Satalecka, K., Schultz, C., Schweizer, T., Shore, S.N., Sillanpää, A., Sitarek, J., Snidaric, I., Sobczynska, D., Stamerra, A., Steinbring, T., Strzys, M., Takalo, L., Takami, H., Tavecchio, F., Temnikov, P., Terzić, T., Tescaro, D., Teshima, M., Thaele, J., Torres, D.F., Toyama, T., Treves, A., Verguilov, V., Vovk, I., Ward, J.E., Will, M., Wu, M.H., Zanin, R., 2016. Long-term multi-wavelength variability and correlation study of Markarian 421 from 2007 to 2009. A&A 593, A91.

Ahnen, M.L., Ansoldi, S., Antonelli, L.A., Arcaro, C., Babić, A., Banerjee, B., Bangale, P., Barres de Almeida, U., Barrio, J.A., Becerra González, J., et al., 2018. Extreme HBL behavior of Markarian 501 during 2012. A&A 620, A181.

Ajello, M., Alexander, D.M., Greiner, J., Madejski, G.M., Gehrels, N., Burlon, D., 2012. The 60 Month All-sky Burst Alert Telescope Survey of Active Galactic Nucleus and the Anisotropy of nearby AGNs. ApJ 749 (1), 21.

Antonucci, R., Kinney, A.L., Hurt, T., 1993. Hubble Space Telescope ultraviolet spectroscopy of the highly polarized but quiescent quasar OI 287. ApJ 414, 506–509.

Archer, A., Benbow, W., Bird, R., Brose, R., Buchovecky, M., Bugaev, V., Cui, W., Daniel, M.K., Falcone, A., Feng, Q., Finley, J.P., Flinders, A., Fortson, L., Furniss, A., Gillanders, G.H., Hütten, M., Hanna, D., Hervet, O., Holder, J., Hughes, G., Humensky, T.B., Johnson, C.A., Kaaret, P., Kar, P., Kelley-Hoskins, N., Kieda, D., Krause, M., Krennrich, F., Kumar, S., Lang, M.J., Lin, T.T.Y., McArthur, S., Moriarty, P., Mukherjee, R., Nieto, D., O'Brien, S., Ong, R.A., Otte, A.N., Park, N., Petrashyk, A., Pohl, M., Popkow, A., Pueschel, E., Quinn, J., Ragan, K., Reynolds, P.T., Richards, G.T., Roache, E., Rulten, C., Sadeh, I., Sembroski, G.H., Shahinyan, K., Tyler, J., Wakely, S.P., Weiner, O.M., Weinstein, A., Wells, R.M., Wilcox, P., Wilhelm, A., Williams, D.A., VERITAS Collaboration, Brisken, W.F., Pontrelli, P., 2018. HESS J1943 + 213: An Extreme Blazar Shining through the Galactic Plane. ApJ 862 (1), 41. https://doi.org/10.3847/1538-4357/aacbd0.

Baloković, M., Paneque, D., Madejski, G., Furniss, A., Chiang, J., Ajello, M., Alexander, D.M., Barret, D., Blandford, R.D., Boggs, S.E., et al., 2016. Multiwavelength Study of Quiescent States of Mrk 421 with Unprecedented Hard X-Ray Coverage Provided by NuSTAR in 2013. ApJ 819 (2), 156.

Barger, A.J., Cowie, L.L., Mushotzky, R.F., Yang, Y., Wang, W.H., Steffen, A.T., Capak, P., 2005. The Cosmic Evolution of Hard X-Ray-selected Active Galactic Nuclei. AJ 129 (2), 578–609.

Barthelmy, S.D., Barbier, L.M., Cummings, J.R., Fenimore, E.E., Gehrels, N., Hullinger, D., Krimm, H.A., Markwardt, C.B., Palmer, D.M., Parsons, A., et al., 2005. The burst alert telescope (bat) on the swift midex mission. Space Science Reviews 120 (3-4), 143–164.

Bassani, L., Alizia, A., Stephen, J.B., 2004. Looking for AGN in the INTEGRAL Core Program. In: Paillé, J.-P. (Ed.), 35th COSPAR Scientific Assembly. COSPAR Meeting 35. pp. 4369.

Bassani, L., Landi, R., Malizia, A., Fiocchi, M.T., Bazzano, A., Bird, A.J., Dean, A.J., Gehrels, N., Giommi, P., Ubertini, P., 2007. IGR J22517 + 2218 = MG3 J225155 + 2217: A New Gamma-Ray Lighthouse in the Distant Universe. ApJ 669 (1), L1–L4.

Bassani, L., Landi, R., Marshall, F.E., Malizia, A., Bazzano, A., Bird, A.J., Gehrels, N., Ubertini, P., Masetti, N., 2012. IGR J12319-0749: evidence for another extreme blazar found with INTEGRAL. A&A 543, A1. https://doi.org/10.1051/0004-6361/201219243.

Bassani, L., Malizia, A., Stephen, J.B., Gianotti, F., Schiavone, F., Bazzano, a., Bird, A.J., Bouchet, L., Courvoisier, T., Dean, A.J., De Cesare, G., Del Santo, M., De Rosa, A., Hudec, R., Mirabel, F., Laurent, P., Piro, L., Shaw, S., Zdziarski, A.A., 2004. The Sky Behind Our Galaxy as Seen by IBIS on INTEGRAL. In: Schoenfelder, V., Lichti, G., Winkler, C. (Eds.), 5th INTEGRAL Workshop on the INTEGRAL Universe. ESA Special Publication 552. pp. 139 astro-ph/0404442.

Bassani, L., Molina, M., Landi, R., Malizia, A., Bird, A.J., Bazzano, A., Ubertini, P., 2013. Chasing extreme blazars with INTEGRAL. arXiv e-prints. arXiv:1302.2447

Bassani, L., Molina, M., Malizia, A., Stephen, J.B., Bird, A.J., Bazzano, A., Bélanger, G., Dean, A.J., De Rosa, A., Laurent, P., Lebrun, F., Ubertini, P., Walter, R., 2006. INTEGRAL IBIS Extragalactic Survey: Active Galactic Nuclei Selected at 20-100 keV. ApJ 636 (2), L65–L68. https://doi.org/10.1086/500132.

Bassani, L., Venturi, T., Molina, M., Malizia, A., Dallacasa, D., Panessa, F., Bazzano, A., Ubertini, P., 2016. Soft γ-ray selected radio galaxies: favouring giant size discovery. MNRAS 461 (3), 3165–3171.

Bazzano, A., Stephen, J.B., Fiocchi, M., Bird, A.J., Bassani, L., Dean, A.J., Malizia, A., Ubertini, P., Lebrun, F., Walter, R., 2006. INTEGRAL IBIS Census of the Sky Beyond 100 keV. ApJ 649 (1), L9–L12.

Beckmann, V., Barthelmy, S.D., Courvoisier, T.J.L., Gehrels, N., Soldi, S., Tueller, J., Wendt, G., 2007. Hard X-ray variability of active galactic nuclei. A&A 475 (3), 827–835.

Beckmann, V., Do Cao, O., 2010. The elusive radio loud Seyfert 2 galaxy NGC 2110. Eighth Integral Workshop. The Restless Gamma-ray Universe (INTEGRAL 2010). pp. 81 1102.4974.

Beckmann, V., Gehrels, N., Favre, P., Walter, R., Courvoisier, T.J.L., Petrucci, P.O.,

Malzac, J., 2004. INTEGRAL and XMM-Newton Spectral Studies of NGC 4388. ApJ 614 (2), 641–647.
Beckmann, V., Jean, P., Lubiński, P., Soldi, S., Terrier, R., 2011. The hard X-ray emission of Centaurus A. A&A 531, A70.
Beckmann, V., Shrader, C.R., Gehrels, N., Soldi, S., Lubiński, P., Zdziarski, A.A., Petrucci, P., Malzac, J., 2005. The high energy spectrum of ngc 4151. The Astrophysical Journal 634 (2), 939–946.
Beckmann, V., Soldi, S., Ricci, C., Alfonso-Garzón, J., Courvoisier, T.J.L., Domingo, A., Gehrels, N., Lubiński, P., Mas-Hesse, J.M., Zdziarski, A.A., 2009. The second INTEGRAL AGN catalogue. A&A 505 (1), 417–439.
Beckmann, V., Soldi, S., Shrader, C.R., Gehrels, N., Produit, N., 2006. The hard xray 20–40 kev agn luminosity function. The Astrophysical Journal 652 (1), 126–135.
Benbow, W., VERITAS Collaboration, 2017. Highlights from the VERITAS AGN Observation Program. International Cosmic Ray Conference 301, 641.
Bianchin, V., Foschini, L., Ghisellini, G., Tagliaferri, G., Tavecchio, F., Treves, A., Di Cocco, G., Gliozzi, M., Pian, E., Sambruna, R.M., Wolter, A., 2009. The changing look of PKS 2149-306. A&A 496 (2), 423–428.
Bikmaev, I.F., Burenin, R.A., Revnivtsev, M.G., Sazonov, S.Y., Sunyaev, R.A., Pavlinsky, M.N., Sakhibullin, N.A., 2008. Optical identifications of five integral hard x-ray sources in the galactic plane. Astronomy Letters 34 (10), 653–663.
Bikmaev, I.F., Sunyaev, R.A., Revnivtsev, M.G., Burenin, R.A., 2006. New nearby active galactic nuclei among integral and rxte x-ray sources. Astronomy Letters 32 (4), 221–227.
Bird, A.J., Barlow, E.J., Bassani, L., Bazzano, A., Belanger, G., Bodaghee, A., Capitanio, F., Dean, A.J., Fiocchi, M., Hill, A.B., et al., 2006. The second ibis/isgri soft gamma ray survey catalog. The Astrophysical Journal 636 (2), 765–776.
Bird, A.J., Barlow, E.J., Bassani, L., Bazzano, A., Bodaghee, A., Capitanio, F., Cocchi, M., Del Santo, M., Dean, A.J., Hill, A.B., et al., 2004. The first ibis/isgri soft gamma-ray galactic plane survey catalog. The Astrophysical Journal 607 (1), L33–L37.
Bird, A.J., Bazzano, A., Bassani, L., Capitanio, F., Fiocchi, M., Hill, A.B., Malizia, A., McBride, V.A., Scaringi, S., Sguera, V., et al., 2009. The fourth ibis/isgri soft gamma-ray survey catalog. The Astrophysical Journal Supplement Series 186 (1), 1–9.
Bird, A.J., Bazzano, A., Malizia, A., Fiocchi, M., Sguera, V., Bassani, L., Hill, A.B., Ubertini, P., Winkler, C., 2016. The ibis soft gamma-ray sky after 1000integralorbits. The Astrophysical Journal Supplement Series 223 (1), 15.
Bird, A.J., Malizia, A., Bazzano, A., Barlow, E.J., Bassani, L., Hill, A.B., Belanger, G., Capitanio, F., Clark, D.J., Dean, A.J., et al., 2007. The third ibis/isgri soft gamma ray survey catalog. The Astrophysical Journal Supplement Series 170 (1), 175–186.
Boettcher, M., 2010. Models for the Spectral Energy Distributions and Variability of Blazars. arXiv e-prints. arXiv:1006.5048
Bottacini, E., Ajello, M., Greiner, J., Pian, E., Rau, A., Palazzi, E., Covino, S., Ghisellini, G., Krühler, T., Küpcü Yoldas, A., Cappelluti, N., Afonso, P., 2010. PKS 0537-286, carrying the information of the environment of SMBHs in the early Universe. A&A 509, A69.
Bottacini, E., Böttcher, M., Pian, E., Collmar, W., 2016. 3C 279 in Outburst in 2015 June: A Broadband SED Study Based on the INTEGRAL Detection. ApJ 832 (1), 17.
Bottacini, E., Böttcher, M., Schady, P., Rau, A., Zhang, X.L., Ajello, M., Fendt, C., Greiner, J., 2010. Probing the Transition Between the Synchrotron and Inverse-compton Spectral Components of 1ES 1959+650. ApJ 719 (2), L162–L166.
Bouchet, L., Jourdain, E., Roques, J., Strong, A., Diehl, R., Lebrun, F., Terrier, R., 2008. Integralspi all sky view in soft gamma rays: A study of point source and galactic diffuse emission. The Astrophysical Journal 679 (2), 1315–1326.
Bruni, G., Panessa, F., Bassani, L., Chiaraluce, E., Kraus, A., Dallacasa, D., Bazzano, A., Hernández-García, L., Malizia, A., Ubertini, P., Ursini, F., Venturi, T., 2019. A Discovery of Young Radio Sources in the Cores of Giant Radio Galaxies Selected at Hard X-Rays. ApJ 875 (2), 88.
Burlon, D., Ajello, M., Greiner, J., Comastri, A., Merloni, A., Gehrels, N., 2011. Three-year Swift-BAT Survey of Active Galactic Nuclei: Reconciling Theory and Observations? ApJ 728 (1), 58.
Buttiglione, S., Capetti, A., Celotti, A., Axon, D.J., Chiaberge, M., Macchetto, F.D., Sparks, W.B., 2010. An optical spectroscopic survey of the 3CR sample of radio galaxies with z < 0.3. II. Spectroscopic classes and accretion modes in radio-loud AGN. A&A 509, A6.
Castignani, G., Pian, E., Belloni, T.M., D'Ammand o, F., Foschini, L., Ghisellini, G., Pursimo, T., Bazzano, A., Beckmann, V., Bianchin, V., Fiocchi, M.T., Impiombato, D., Raiteri, C.M., Soldi, S., Tagliaferri, G., Treves, A., Türler, M., 2017. Multiwavelength variability study and search for periodicity of PKS 1510-089. A&A 601, A30.
Chevalier, J., Sanchez, D.A., Serpico, P.D., Lenain, J.P., Maurin, G., 2019. Variability studies and modelling of the blazar PKS 2155-304 in the light of a decade of multi-wavelength observations. MNRAS 484 (1), 749–759.
Chiaro, G., Salvetti, D., La Mura, G., Giroletti, M., Thompson, D.J., Bastieri, D., 2016. Blazar flaring patterns (B-FlaP) classifying blazar candidate of uncertain type in the third Fermi-LAT catalogue by artificial neural networks. MNRAS 462 (3), 3180–3195.
Collmar, W., Böttcher, M., Krichbaum, T.P., Agudo, I., Bottacini, E., Bremer, M., Burwitz, V., Cuccchiara, A., Grupe, D., Gurwell, M., 2010. The multifrequency campaign on 3C 279 in January 2006. A&A 522, A66.
Comastri, A., Gilli, R., Hasinger, G., 2006. Rolling down from the 30 kev peak: Modelling the hard x-ray and I-ray backgrounds. Experimental Astronomy 20 (1-3), 41–47.
Comastri, A., Mignoli, M., Ciliegi, P., Severgnini, P., Maiolino, R., Brusa, M., Fiore, F., Baldi, A., Molendi, S., Morganti, R., Vignali, C., La Franca, F., Matt, G., Perola, G.C., 2002. The HELLAS2XMM Survey. II. Multiwavelength Observations of P3: An X-Ray-bright, Optically Inactive Galaxy. ApJ 571 (2), 771–778.
Costamante, L., Cutini, S., Tosti, G., Antolini, E., Tramacere, A., 2018. On the origin of gamma-rays in Fermi blazars: beyondthe broad-line region. MNRAS 477 (4), 4749–4767.
Dadina, M., 2007. BeppoSAX observations in the 2-100 keV band of the nearby Seyfert galaxies: an atlas of spectra. A&A 461 (3), 1209–1252.
de Rosa, A., Bassani, L., Ubertini, P., Malizia, A., Dean, A.J., 2008. Bulk Compton motion in the luminous quasar 4C04.42? MNRAS 388 (1), L54–L58. https://doi.org/10.1111/j.1745-3933.2008.00498.x.
de Rosa, A., Panessa, F., Bassani, L., Bazzano, A., Bird, A., Landi, R., Malizia, A., Molina, M., Ubertini, P., 2012. Broad-band study of hard X-ray-selected absorbed active galactic nuclei. MNRAS 420 (3), 2087–2101.
Fabian, A.C., Lohfink, A., Belmont, R., Malzac, J., Coppi, P., 2017. Properties of AGN coronae in the NuSTAR era - II. Hybrid plasma. MNRAS 467 (3), 2566–2570. https://doi.org/10.1093/mnras/stx221.
Fabian, A.C., Lohfink, A., Kara, E., Parker, M.L., Vasudevan, R., Reynolds, C.S., 2015. Properties of AGN coronae in the NuSTAR era. MNRAS 451 (4), 4375–4383. https://doi.org/10.1093/mnras/stv1218.
Falomo, R., Pian, E., Treves, A., 2014. An optical view of BL Lacertae objects. A&ARv 22, 73.
Fan, J.H., Yang, J.H., Liu, Y., Luo, G.Y., Lin, C., Yuan, Y.H., Xiao, H.B., Zhou, A.Y., Hua, T.X., Pei, Z.Y., 2016. The Spectral Energy Distributions of Fermi Blazars. ApJS 226 (2), 20.
Fanaroff, B.L., Riley, J.M., 1974. The morphology of extragalactic radio sources of high and low luminosity. MNRAS 167, 31P–36P.
Fedorova, E.V., Beckmann, V., Neronov, A., Soldi, S., 2011. Studying the long-time variability of the Seyfert 2 galaxy NGC 4388 with INTEGRAL and Swift. MNRAS 417 (2), 1140–1147.
Fedorova, E.V., Zhdanov, V.I., 2016. Variations of the X-ray INTEGRAL spectrum of the active galactic nucleus of NGC 4945. Kinematics and Physics of Celestial Bodies 32 (4), 172–180.
Foffano, L., Prandini, E., Franceschini, A., Paiano, S., 2019. A new hard X-ray-selected sample of extreme high-energy peaked BL Lac objects and their TeV gamma-ray properties. MNRAS 486 (2), 1741–1762. https://doi.org/10.1093/mnras/stz812.
Fossati, G., Maraschi, L., Celotti, A., Comastri, A., Ghisellini, G., 1998. A unifying view of the spectral energy distributions of blazars. MNRAS 299 (2), 433–448.
Frontera, F., Costa, E., Dal Fiume, D., Feroci, M., Nicastro, L., Orlandini, M., Palazzi, E., Zavattini, G., 1997. The high energy instrument pds on-board the bepposax x–ray astronomy satellite. Astronomy and Astrophysics Supplement Series 122 (2), 357–369.
Furniss, A., Noda, K., Boggs, S., Chiang, J., Christensen, F., Craig, W., Giommi, P., Hailey, C., Harisson, F., Madejski, G., et al., 2015. First NuSTAR Observations of Mrk 501 within a Radio to TeV Multi-Instrument Campaign. ApJ 812 (1), 65.
Gao, S., Fedynitch, A., Winter, W., Pohl, M., 2019. Modelling the coincident observation of a high-energy neutrino and a bright blazar flare. Nature Astronomy 3, 88–92.
Ghisellini, G., Celotti, A., Fossati, G., Maraschi, L., Comastri, A., 1998. A theoretical unifying scheme for gamma-ray bright blazars. MNRAS 301 (2), 451–468.
Ghisellini, G., Foschini, L., Tavecchio, F., Pian, E., 2007. On the 2007 July flare of the blazar 3C 454.3. MNRAS 382 (1), L82–L86.
Gianní, S., de Rosa, A., Bassani, L., Bazzano, A., Dean, T., Ubertini, P., 2011. An X-ray view of the INTEGRAL/IBIS blazars. MNRAS 411 (4), 2137–2147.
Gilli, R., Comastri, A., Hasinger, G., 2007. The synthesis of the cosmic X-ray background in the Chandra and XMM-Newton era. A&A 463 (1), 79–96. https://doi.org/10.1051/0004-6361:20066334.
Giovannini, G., Giroletti, M., Taylor, G.B., 2007. B2 1144+35B, a giant low power radio galaxy with superluminal motion. Orientation and evidence for recurrent activity. A&A 474 (2), 409–414.
Grebenev, S.A., Lutovinov, A.A., Tsygankov, S.S., Mereminskiy, I.A., 2012. Deep hard x-ray survey of the large magellanic cloud. Monthly Notices of the Royal Astronomical Society 428 (1), 50–57.
H. E. S. S. Collaboration, Abdalla, H., Adam, R., Aharonian, F., Ait Benkhali, F., Angüner, E.O., Arakawa, M., Arcaro, C., Armand, C., Ashkar, H., Backes, M., Barbosa Martins, V., Barnard, M., Becherini, Y., Berge, D., Bernlöhr, K., Blackwell, R., Böttcher, M., Boisson, C., Bolmont, J., Bonnefoy, S., Bregeon, J., Breuhaus, M., Brun, F., Brun, P., Bryan, M., Büchele, M., Bulik, T., Bylund, T., Capasso, M., Caroff, S., Carosi, A., Casanova, S., Cerruti, M., Chand, T., Chandra, S., Chen, A., Colafrancesco, S., Curyło, M., Davids, I.D., Deil, C., Devin, J., deWilt, P., Dirson, L., Djannati-Ataï, A., Dmytriiev, A., Donath, A., Doroshenko, V., Drury, L.O.C., Dyks, J., Egberts, K., Emery, G., Ernenwein, J.P., Eschbach, S., Feijen, K., Fegan, S., Fiasson, A., Fontaine, G., Funk, S., Füßling, M., Gabici, S., Gallant, Y.A., Gaté, F., Giavitto, G., Glawion, D., Glicenstein, J.F., Gottschall, D., Grondin, M.H., Hahn, J., Haupt, M., Heinzelmann, G., Henri, G., Hermann, G., Hinton, J.A., Hofmann, W., Hoischen, C., Holch, T.L., Holler, M., Horns, D., Huber, D., Iwasaki, H., Jamrozy, M., Jankowsky, D., Jankowsky, F., Jardin-Blicq, A., Jung-Richardt, I., Kastendieck, M.A., Katarzyński, K., Katsuragawa, M., Katz, U., Khangulyan, D., Khélifi, B., King, J., Klepser, S., Kluźniak, W., Komin, N., Kosack, K., Kostunin, D., Kraus, M., Lamanna, G., Lau, J., Lemière, A., Lemoine-Goumard, M., Lenain, J.P., Leser, E., Levy, C., Lohse, T., Lypova, I., Mackey, J., Majumdar, J., Malyshev, D., Marandon, V., Marcowith, A., Mares, A., Mariaud, C., Martí-Devesa, G., Marx, R., Maurin, G., Meintjes, P.J., Mitchell, A.M.W., Moderski, R., Mohamed, M., Mohrmann, L., Moore, C., Moulin, E., Muller, J., Murach, T., Nakashima, S., de Naurois, M., Ndiyavala, H., Niederwanger, F., Niemiec, J., Oakes, L., O'Brien, P., Odaka, H., Ohm, S., de Ona Wilhelmi, E., Ostrowski, M., Oya, I., Panter, M., Parsons, R.D., Perennes, C., Petrucci, P.O., Peyaud, B., Piel, Q., Pita, S., Poireau, V., Priyana Noel, A., Prokhorov, D.A., Prokoph, H., Pühlhofer, G., Punch, M., Quirrenbach, A., Raab, S., Rauth, R., Reimer, A., Reimer, O., Remy, Q., Renaud, M., Rieger, F., Rinchiuso, L., Romoli, C., Rowell, G., Rudak, B., Ruiz-Velasco, E., Sahakian, V., Saito, S., Sanchez, D.A., Santangelo, A., Sasaki, M., Schlickeiser, R., Schüssler, F., Schulz, A., Schutte, H., Schwanke, U., Schwemmer, S., Seglar-Arroyo, M., Senniappan, M., Seyffert, A.S., Shafi, N., Shiningayamwe, K., Simoni, R., Sinha, A., Sol, H., Specovius, A., Spir-Jacob, M., Stawarz, L., Steenkamp, R., Stegmann, C., Steppa, C., Takahashi, T., Tavernier, T., Taylor, A.M., Terrier, R., Tiziani, D.,

Tluczykont, M., Trichard, C., Tsirou, M., Tsuji, N., Tuffs, R., Uchiyama, Y., van der Walt, D.J., van Eldik, C., van Rensburg, C., van Soelen, B., Vasileiadis, G., Veh, J., Venter, C., Vincent, P., Vink, J., Voisin, F., Völk, H.J., Vuillaume, T., Wadiasingh, Z., Wagner, S.J., White, R., Wierzcholska, A., Yang, R., Yoneda, H., Zacharias, M., Zanin, R., Zdziarski, A.A., Zech, A., Ziegler, A., Zorn, J., Żywucka, N., Meyer, M., 2019. Constraints on the emission region of <ASTROBJ>3C 279</ASTROBJ> during strong flares in 2014 and 2015 through VHE γ-ray observations with H.E.S.S. A&A 627, A159. https://doi.org/10.1051/0004-6361/201935704.

H. E. S. S. Collaboration, Abramowski, A., Acero, F., Aharonian, F., Akhperjanian, A.G., Anton, G., Balzer, A., Barnacka, A., Barres de Almeida, U., Bazer-Bachi, A.R., Becherini, Y., Becker, J., Behera, B., Bernlöhr, K., Bochow, A., Boisson, C., Bolmont, J., Bordas, P., Borrel, V., Brucker, J., Brun, F., Brun, P., Bulik, T., Büsching, I., Carrigan, S., Casanova, S., Cerruti, M., Chadwick, P.M., Charbonnier, A., Chaves, R.C.G., Cheesebrough, A., Chounet, L.M., Clapson, A.C., Coignet, G., Colom, P., Conrad, J., Dalton, M., Daniel, M.K., Davids, I.D., Degrange, B., Deil, C., Dickinson, H.J., Djannati-Ataï, A., Domainko, W., Drury, L.O.C., Dubois, F., Dubus, G., Dyks, J., Dyrda, M., Egberts, K., Eger, P., Espigat, P., Fallon, L., Farnier, C., Fegan, S., Feinstein, F., Fernandes, M.V., Fiasson, A., Fontaine, G., Förster, A., Füßling, M., Gallant, Y.A., Gast, H., Gérard, L., Gerbig, D., Giebels, B., Glicenstein, J.F., Glück, B., Goret, P., Göring, D., Häffner, S., Hague, J.D., Hampf, D., Hauser, M., Heinz, S., Heinzelmann, G., Henri, G., Hermann, G., Hinton, J.A., Hoffmann, A., Hofmann, W., Hofverberg, P., Holler, M., Horns, D., Jacholkowska, A., de Jager, O.C., Jahn, C., Jamrozy, M., Jung, I., Kastendieck, M.A., Katarzyński, K., Katz, U., Kaufmann, S., Keogh, D., Khangulyan, D., Khélifi, B., Klochkov, D., Kluźniak, W., Kneiske, T., Komin, N., Kosack, K., Kossakowski, R., Laffon, H., Lamanna, G., Lennarz, D., Lohse, T., Lopatin, A., Lu, C.C., Marandon, V., Marcowith, A., Masbou, J., Maurin, D., Maxted, N., McComb, T.J.L., Medina, M.C., Méhault, J., Nguyen, N., Moderski, R., Moulin, E., Naumann, C.L., Naumann-Godo, M., de Naurois, M., Nedbal, D., Nekrassov, D., Nicholas, B., Niemiec, J., Nolan, S.J., Ohm, S., Olive, J.F., de Oña Wilhelmi, E., Opitz, B., Ostrowski, M., Panter, M., Paz Arribas, M., Pedaletti, G., Pelletier, G., Petrucci, P.O., Pita, S., Pühlhofer, G., Punch, M., Quirrenbach, A., Raue, M., Rayner, S.M., Reimer, A., Reimer, O., Renaud, M., de los Reyes, R., Rieger, F., Ripken, J., Rob, L., Rosier-Lees, S., Rowell, G., Rudak, B., Rulten, C.B., Ruppel, J., Ryde, F., Sahakian, V., Santangelo, A., Schlickeiser, R., Schöck, F.M., Schönwald, A., Schulz, A., Schwanke, U., Schwarzburg, S., Schwemmer, S., Shalchi, A., Sikora, M., Skilton, J.L., Sol, H., Spengler, G., Stawarz, Ł., Steenkamp, R., Stegmann, C., Stinzing, F., Stycz, K., Sushch, I., Szostek, A., Tavernet, J.P., Terrier, R., Tibolla, O., Tluczykont, M., Valerius, K., van Eldik, C., Vasileiadis, G., Venter, C., Vialle, J.P., Viana, A., Vincent, P., Vivier, M., Völk, H.J., Volpe, F., Vorobiov, S., Vorster, M., Wagner, S.J., Ward, M., Wierzcholska, A., Zajczyk, A., Zdziarski, A.A., Zech, A., Zechlin, H.S., Burnett, T.H., Hill, A.B., 2011. HESS J1943+213: a candidate extreme BL Lacertae object. A&A 529, A49. https://doi.org/10.1051/0004-6361/201116545.

Harrison, F.A., Aird, J., Civano, F., Lansbury, G., Mullaney, J.R., Ballantyne, D.R., Alexander, D.M., Stern, D., Ajello, M., Barret, D., Bauer, F.E., Baloković, M., Brandt, W.N., Brightman, M., Boggs, S.E., Christensen, F.E., Comastri, A., Craig, W.W., Del Moro, A., Forster, K., Gandhi, P., Giommi, P., Grefenstette, B.W., Hailey, C.J., Hickox, R.C., Hornstrup, A., Kitaguchi, T., Koglin, J., Luo, B., Madsen, K.K., Mao, P.H., Miyasaka, H., Mori, K., Perri, M., Pivovaroff, M., Puccetti, S., Rana, V., Treister, E., Walton, D., Westergaard, N.J., Wik, D., Zappacosta, L., Zhang, W.W., Zoglauer, A., 2016. The NuSTAR Extragalactic Surveys: The Number Counts of Active Galactic Nuclei and the Resolved Fraction of the Cosmic X-Ray Background. ApJ 831 (2), 185.

Hönig, S.F., 2019. Redefining the Torus: A Unifying View of AGNs in the Infrared and Submillimeter. ApJ 884 (2), 171. https://doi.org/10.3847/1538-4357/ab4591.

IceCube Collaboration, Aartsen, M.G., Ackermann, M., Adams, J., Aguilar, J.A., Ahlers, M., Ahrens, M., Al Samarai, I., Altmann, D., Andeen, K., et al., 2018. Multimessenger observations of a flaring blazar coincident with high-energy neutrino IceCube-170922A. Science 361 (6398), eaat1378.

Karasev, D.I., Lutovinov, A.A., Tkachenko, A.Y., Khorunzhev, G.A., Krivonos, R.A., Medvedev, P.S., Pavlinsky, M.N., Burenin, R.A., Eselevich, M.V., 2018. Optical identification of x-ray sources from the 14-year integral all-sky survey. Astronomy Letters 44 (8-9), 522–540.

Keivani, A., Murase, K., Petropoulou, M., Fox, D.B., Cenko, S.B., Chaty, S., Coleiro, A., DeLaunay, J.J., Dimitrakoudis, S., Evans, P.A., Kennea, J.A., Marshall, F.E., Mastichiadis, A., Osborne, J.P., Santand er, M., Tohuvavohu, A., Turley, C.F., 2018. A Multimessenger Picture of the Flaring Blazar TXS 0506+056: Implications for High-energy Neutrino Emission and Cosmic-Ray Acceleration. ApJ 864 (1), 84.

Khorunzhev, G.A., Sazonov, S.Y., Burenin, R.A., Tkachenko, A.Y., 2012. Masses and accretion rates of supermassive black holes in active galactic nuclei from the INTEGRAL survey. Astronomy Letters 38 (8), 475–491.

Krawczynski, H., Hughes, S.B., Horan, D., Aharonian, F., Aller, M.F., Aller, H., Boltwood, P., Buckley, J., Coppi, P., Fossati, G., Götting, N., Holder, J., Horns, D., Kurtanidze, O.M., Marscher, A.P., Nikolashvili, M., Remillard, R.A., Sadun, A., Schröder, M., 2004. Multiwavelength Observations of Strong Flares from the TeV Blazar 1ES 1959+650. ApJ 601 (1), 151–164.

Krivonos, R., Revnivtsev, M., Lutovinov, A., Sazonov, S., Churazov, E., Sunyaev, R., 2007. INTEGRAL/IBIS all-sky survey in hard X-rays. A&A 475 (2), 775–784.

Krivonos, R., Tsygankov, S., Lutovinov, A., Revnivtsev, M., Churazov, E., Sunyaev, R., 2015. INTEGRAL 11-year hard X-ray survey above 100 keV. MNRAS 448 (4), 3766–3774.

Landi, R., Bassani, L., Bazzano, A., Bird, A.J., Fiocchi, M., Malizia, A., Panessa, F., Sguera, V., Ubertini, P., 2017. Investigating the X-ray counterparts to unidentified sources in the 1000-orbit INTEGRAL/IBIS catalogue. MNRAS 470 (1), 1107–1120. https://doi.org/10.1093/mnras/stx908.

Landi, R., Bassani, L., Malizia, A., Stephen, J.B., Bazzano, A., Fiocchi, M., Bird, A.J., 2010. Swift/xrt observations of unidentified integral/ibis sources. Monthly Notices of the Royal Astronomical Society 403 (2), 945–959.

Landi, R., Stephen, J.B., Masetti, N., Grupe, D., Capitanio, F., Bird, A.J., Dean, A.J., Fiocchi, M., Gehrels, N., 2009. The AGN nature of three INTEGRAL sources: IGR J18249-3243, IGR J19443+2117, and IGR J22292+6647. A&A 493 (3), 893–898. https://doi.org/10.1051/0004-6361:200810503.

Lanzuisi, G., de Rosa, A., Ghisellini, G., Ubertini, P., Panessa, F., Ajello, M., Bassani, L., Fukazawa, Y., D'Ammando, F., 2012. Modelling the flaring activity of the high-z, hard X-ray-selected blazar IGR J22517+2217. MNRAS 421 (1), 390–397.

Levine, A.M., Lang, F.L., Lewin, W.H.G., Primini, F.A., Dobson, C.A., Doty, J.P., Hoffman, J.A., Howe, S.K., Scheepmaker, A., Wheaton, W.A., et al., 1984. The heao 1 a-4 catalog of high-energy x-ray sources. The Astrophysical Journal Supplement Series 54, 581.

Lichti, G.G., Bottacini, E., Ajello, M., Charlot, P., Collmar, W., Falcone, A., Horan, D., Huber, S., von Kienlin, A., Lähteenmäki, A., Lindfors, E., Morris, D., Nilsson, K., Petry, D., Rüger, M., Sillanpää, A., Spanier, F., Tornikoski, M., 2008. INTEGRAL observations of the blazar Mrk 421 in outburst. Results of a multi-wavelength campaign. A&A 486 (3), 721–734.

Lubiński, P., Beckmann, V., Gibaud, L., Paltani, S., Papadakis, I.E., Ricci, C., Soldi, S., Türler, M., Walter, R., Zdziarski, A.A., 2016. A comprehensive analysis of the hard X-ray spectra of bright Seyfert galaxies. MNRAS 458 (3), 2454–2475.

Lubiński, P., Zdziarski, A.A., Walter, R., Paltani, S., Beckmann, V., Soldi, S., Ferrigno, C., Courvoisier, T.J.L., 2010. Extreme flux states of NGC 4151 observed with INTEGRAL. MNRAS 408 (3), 1851–1865.

Luo, B., Brandt, W.N., Xue, Y.Q., Lehmer, B., Alexander, D.M., Bauer, F.E., Vito, F., Yang, G., Basu-Zych, A.R., Comastri, A., Gilli, R., Gu, Q.S., Hornschemeier, A.E., Koekemoer, A., Liu, T., Mainieri, V., Paolillo, M., Ranalli, P., Rosati, P., Schneider, D.P., Shemmer, O., Smail, I., Sun, M., Tozzi, P., Vignali, C., Wang, J.X., 2017. The Chandra Deep Field-South Survey: 7 Ms Source Catalogs. ApJS 228 (1), 2.

MacDonald, J., Mullan, D.J., 2017. Magnetic Modeling of Inflated Low-mass Stars Using Interior Fields No Larger than Ì10 kG. ApJ 850 (1), 58.

Maiolino, R., Rieke, G.H., 1995. Low-Luminosity and Obscured Seyfert Nuclei in Nearby Galaxies. ApJ 454, 95.

Malizia, A., Bassani, L., Bazzano, A., Bird, A.J., Masetti, N., Panessa, F., Stephen, J.B., Ubertini, P., 2012. The INTEGRAL/IBIS AGN catalogue - I. X-ray absorption properties versus optical classification. MNRAS 426 (3), 1750–1766. https://doi.org/10.1111/j.1365-2966.2012.21755.x.

Malizia, A., Bassani, L., Bird, A.J., Landi, R., Masetti, N., de Rosa, A., Panessa, F., Molina, M., Dean, A.J., Perri, M., Tueller, J., 2008. First high-energy observations of narrow-line Seyfert 1s with INTEGRAL/IBIS. MNRAS 389 (3), 1360–1366.

Malizia, A., Bassani, L., Stephen, J.B., Di Cocco, G., Fiore, F., Dean, A.J., 2003. BeppoSAX Average Spectra of Seyfert Galaxies. ApJ 589 (1), L17–L20.

Malizia, A., Landi, R., Bassani, L., Bird, A.J., Molina, M., De Rosa, A., Fiocchi, M., Gehrels, N., Kennea, J., Perri, M., 2007. Swiftxrt observation of 34 newintegralibis agns: Discovery of compton thick and other peculiar sources. The Astrophysical Journal 668 (1), 81–86.

Malizia, A., Landi, R., Molina, M., Bassani, L., Bazzano, A., Bird, A.J., Ubertini, P., 2016. The integral/ibisagn catalogue: an update. Monthly Notices of the Royal Astronomical Society 460 (1), 19–29.

Malizia, A., Molina, M., Bassani, L., Stephen, J.B., Bazzano, A., Ubertini, P., Bird, A.J., 2014. The INTEGRAL High-energy Cut-off Distribution of Type 1 Active Galactic Nuclei. ApJ 782 (2), L25.

Malizia, A., Stephen, J.B., Bassani, L., Bird, A.J., Panessa, F., Ubertini, P., 2009. The fraction of Compton-thick sources in an INTEGRAL complete AGN sample. MNRAS 399 (2), 944–951.

Maraschi, L., Haardt, F., 1997. Disk-Corona Models and X-Ray Emission from Seyfert Galaxies. In: Wickramasinghe, D.T., Bicknell, G.V., Ferrario, L. (Eds.), IAU Colloq. 163: Accretion Phenomena and Related Outflows. Astronomical Society of the Pacific Conference Series 121. pp. 101 astro-ph/9611048.

Markwardt, C.B., Tueller, J., Skinner, G.K., Gehrels, N., Barthelmy, S.D., Mushotzky, R.F., 2005. The Swift/BAT High-Latitude Survey: First Results. ApJ 633 (2), L77–L80.

Masetti, N., Mason, E., Landi, R., Giommi, P., Bassani, L., Malizia, A., Bird, A.J., Bazzano, A., Dean, A.J., Gehrels, N., Palazzi, E., Ubertini, P., 2008. High-redshift blazar identification for Swift J1656.3-3302. A&A 480 (3), 715–721. https://doi.org/10.1051/0004-6361:20078901.

Masetti, N., Mason, E., Morelli, L., Cellone, S.A., McBride, V.A., Palazzi, E., Bassani, L., Bazzano, A., Bird, A.J., Charles, P.A., Dean, A.J., Galaz, G., Gehrels, N., Landi, R., Malizia, A., Minniti, D., Panessa, F., Romero, G.E., Stephen, J.B., Ubertini, P., Walter, R., 2008. Unveiling the nature of INTEGRAL objects through optical spectroscopy. VI. A multi-observatory identification campaign. A&A 482 (1), 113–132. https://doi.org/10.1051/0004-6361:20079332.

Mathur, S., 2000. Narrow-line Seyfert 1 galaxies and the evolution of galaxies and active galaxies. MNRAS 314 (4), L17–L20.

Mereminskiy, I.A., Krivonos, R.A., Lutovinov, A.A., Sazonov, S.Y., Revnivtsev, M.G., Sunyaev, R.A., 2016. Integral/ibis deep extragalactic survey: M81, lmc and 3c 273/coma fields. Monthly Notices of the Royal Astronomical Society 459 (1), 140–150.

Molina, M., Bassani, L., Malizia, A., Bird, A.J., Bazzano, A., Ubertini, P., Venturi, T., 2014. IGR J17488-2338: a newly discovered giant radio galaxy. A&A 565, A2.

Molina, M., Bassani, L., Malizia, A., Stephen, J.B., Bird, A.J., Bazzano, A., Ubertini, P., 2013. Hard-X-ray spectra of active galactic nuclei in the INTEGRAL complete sample.

MNRAS 433 (2), 1687–1700.
Molina, M., Malizia, A., Bassani, L., Bird, A.J., Dean, A.J., Landi, R., de Rosa, A., Walter, R., Barlow, E.J., Clark, D.J., 2006. INTEGRAL observations of active galactic nuclei obscured by the Galactic plane. MNRAS 371 (2), 821–828.
Molina, M., Malizia, A., Bassani, L., Ursini, F., Bazzano, A., Ubertini, P., 2019. Swift/XRT-NuSTAR spectra of type 1 AGN: confirming INTEGRAL results on the high-energy cut-off. MNRAS 484 (2), 2735–2746.
Molina, M., Venturi, T., Malizia, A., Bassani, L., Dallacasa, D., Lal, D.V., Bird, A.J., Ubertini, P., 2015. IGR J14488-4008: an X-ray peculiar giant radio galaxy discovered by INTEGRAL. MNRAS 451 (3), 2370–2375.
Murase, K., 2017. Active Galactic Nuclei as High-Energy Neutrino Sources. pp. 15–31.
Oh, K., Koss, M., Markwardt, C.B., Schawinski, K., Baumgartner, W.H., Barthelmy, S.D., Cenko, S.B., Gehrels, N., Mushotzky, R., Petulante, A., et al., 2018. The 105-month swift-bat all-sky hard x-ray survey. The Astrophysical Journal Supplement Series 235 (1), 4.
Osterbrock, D.E., Pogge, R.W., 1985. The spectra of narrow-line Seyfert 1 galaxies. ApJ 297, 166–176.
Padovani, P., Giommi, P., Rau, A., 2012. The discovery of high-power high synchrotron peak blazars. MNRAS 422 (1), L48–L52.
Panessa, F., Bassani, L., de Rosa, A., Bird, A.J., Dean, A.J., Fiocchi, M., Malizia, A., Molina, M., Ubertini, P., Walter, R., 2008. The broad-band XMM-Newton and INTEGRAL spectra of bright type 1 Seyfert galaxies. A&A 483 (1), 151–160.
Panessa, F., Bassani, L., Landi, R., Bazzano, A., Dallacasa, D., La Franca, F., Malizia, A., Venturi, T., Ubertini, P., 2016. The column density distribution of hard X-ray radio galaxies. MNRAS 461 (3), 3153–3164.
Panessa, F., de Rosa, A., Bassani, L., Bazzano, A., Bird, A., Landi, R., Malizia, A., Miniutti, G., Molina, M., Ubertini, P., 2011. Narrow-line Seyfert 1 galaxies at hard X-rays. MNRAS 417 (4), 2426–2439. https://doi.org/10.1111/j.1365-2966.2011.19268.x.
Panessa, F., Tarchi, A., Castangia, P., Maiorano, E., Bassani, L., Bicknell, G., Bazzano, A., Bird, A.J., Malizia, A., Ubertini, P., 2015. The 1.4-GHz radio properties of hard X-ray-selected AGN. MNRAS 447 (2), 1289–1298. https://doi.org/10.1093/mnras/stu2455.
Perola, G.C., Matt, G., Cappi, M., Fiore, F., Guainazzi, M., Maraschi, L., Petrucci, P.O., Piro, L., 2002. Compton reflection and iron fluorescence in BeppoSAX observations of Seyfert type 1 galaxies. A&A 389, 802–811.
Petrucci, P.O., Haardt, F., Maraschi, L., Grandi, P., Malzac, J., Matt, G., Nicastro, F., Piro, L., Perola, G.C., De Rosa, A., 2001. Testing Comptonization Models Using BeppoSAX Observations of Seyfert 1 Galaxies. ApJ 556 (2), 716–726.
Pian, E., Foschini, L., Beckmann, V., Sillanpää, A., Soldi, S., Tagliaferri, G., Takalo, L., Barr, P., Ghisellini, G., Malaguti, G., Maraschi, L., Palumbo, G.G.C., Treves, A., Courvoisier, T.J.L., Di Cocco, G., Gehrels, N., Giommi, P., Hudec, R., Lindfors, E., Marcowith, A., Nilsson, K., Pasanen, M., Pursimo, T., Raiteri, C.M., Savolainen, T., Sikora, M., Tornikoski, M., Tosti, G., Türler, M., Valtaoja, E., Villata, M., Walter, R., 2005. INTEGRAL observations of the field of the BL Lacertae object S5 0716+714. A&A 429, 427–431.
Pian, E., Foschini, L., Beckmann, V., Soldi, S., Türler, M., Gehrels, N., Ghisellini, G., Giommi, P., Maraschi, L., Pursimo, T., Raiteri, C.M., Tagliaferri, G., Tornikoski, M., Tosti, G., Treves, A., Villata, M., Barr, P., Courvoisier, T.J.L., Di Cocco, G., Hudec, R., Fuhrmann, L., Malaguti, G., Persic, M., Tavecchio, F., Walter, R., 2006. INTEGRAL observations of the blazar 3C 454.3 in outburst. A&A 449 (2), L21–L25.
Pian, E., Türler, M., Fiocchi, M., Boissay, R., Bazzano, A., Foschini, L., Tavecchio, F., Bianchin, V., Castignani, G., Ferrigno, C., Raiteri, C.M., Villata, M., Beckmann, V., D'Ammand o, F., Hudec, R., Malaguti, G., Maraschi, L., Pursimo, T., Romano, P., Soldi, S., Stamerra, A., Treves, A., Ubertini, P., Vercellone, S., Walter, R., 2014. An active state of the BL Lacertae object Markarian 421 detected by INTEGRAL in April 2013. A&A 570, A77.
Pian, E., Ubertini, P., Bazzano, A., Beckmann, V., Eckert, D., Ghisellini, G., Pursimo, T., Tagliaferri, G., Tavecchio, F., Türler, M., Bianchi, S., Bianchin, V., Hudec, R., Maraschi, L., Raiteri, C.M., Soldi, S., Treves, A., Villata, M., 2011. INTEGRAL observations of the GeV blazar PKS 1502+106 and the hard X-ray bright Seyfert galaxy Mkn 841. A&A 526, A125.
Pian, E., Vacanti, G., Tagliaferri, G., Ghisellini, G., Maraschi, L., Treves, A., Urry, C.M., Fiore, F., Giommi, P., Palazzi, E., Chiappetti, L., Sambruna, R.M., 1998. BeppoSAX Observations of Unprecedented Synchrotron Activity in the BL Lacertae Object Markarian 501. ApJ 492 (1), L17–L20.
Pounds, K.A., Done, C., Osborne, J.P., 1995. RE 1034+39: a high-state Seyfert galaxy? MNRAS 277 (1), L5–L10.
Ranalli, P., Comastri, A., Vignali, C., Carrera, F.J., Cappelluti, N., Gilli, R., Puccetti, S., Brand t, W.N., Brunner, H., Brusa, M., Georgantopoulos, I., Iwasawa, K., Mainieri, V., 2013. The XMM deep survey in the CDF-S. III. Point source catalogue and number counts in the hard X-rays. A&A 555, A42.
Ricci, C., Trakhtenbrot, B., Koss, M.J., Ueda, Y., Schawinski, K., Oh, K., Lamperti, I., Mushotzky, R., Treister, E., Ho, L.C., et al., 2017. The close environments of accreting massive black holes are shaped by radiative feedback. Nature 549 (7673), 488–491. https://doi.org/10.1038/nature23906.
Ricci, C., Ueda, Y., Koss, M.J., Trakhtenbrot, B., Bauer, F.E., Gandhi, P., 2015. Compton-thick Accretion in the Local Universe. ApJ 815 (1), L13.
Righi, C., Tavecchio, F., Inoue, S., 2019. Neutrino emission from BL Lac objects: the role of radiatively inefficient accretion flows. MNRAS 483 (1), L127–L131.
Risaliti, G., Maiolino, R., Salvati, M., 1999. The Distribution of Absorbing Column Densities among Seyfert 2 Galaxies. ApJ 522 (1), 157–164.
Sambruna, R.M., Maraschi, L., Urry, C.M., 1996. On the Spectral Energy Distributions of Blazars. ApJ 463, 444. https://doi.org/10.1086/177260.
Sazonov, S., Churazov, E., Krivonos, R., 2015. Does the obscured AGN fraction really depend on luminosity? MNRAS 454 (2), 1202–1220.
Sazonov, S., Churazov, E.M., Krivonos, R., Revnivtsev, M., Sunyaev, R., 2010. Statistical properties of local AGN based on the INTEGRAL/IBIS 7-year all-sky hard X-ray survey. Eighth Integral Workshop. The Restless Gamma-ray Universe (INTEGRAL 2010). pp. 6.
Sazonov, S., Krivonos, R., Revnivtsev, M., Churazov, E., Sunyaev, R., 2008. Cumulative hard X-ray spectrum of local AGN: a link to the cosmic X-ray background. A&A 482 (2), 517–527.
Sazonov, S., Revnivtsev, M., Burenin, R., Churazov, E., Sunyaev, R., Forman, W.R., Murray, S.S., 2008. Discovery of heavily-obscured AGN among seven INTEGRAL hard X-ray sources observed by Chandra. A&A 487 (2), 509–517.
Sazonov, S., Revnivtsev, M., Krivonos, R., Churazov, E., Sunyaev, R., 2007. Hard X-ray luminosity function and absorption distribution of nearby AGN: INTEGRAL all-sky survey. A&A 462 (1), 57–66.
Sazonov, S., Willner, S.P., Goulding, A.D., Hickox, R.C., Gorjian, V., Werner, M.W., Churazov, E., Krivonos, R., Revnivtsev, M., Sunyaev, R., Jones, C., Murray, S.S., Vikhlinin, A., Fabian, A.C., Forman, W.R., 2012. Contribution of the Accretion Disk, Hot Corona, and Obscuring Torus to the Luminosity of Seyfert Galaxies: INTEGRAL and Spitzer Observations. ApJ 757 (2), 181.
Sazonov, S.Y., Ostriker, J.P., Sunyaev, R.A., 2004. Quasars: the characteristic spectrum and the induced radiative heating. MNRAS 347 (1), 144–156.
Sazonov, S.Y., Revnivtsev, M.G., 2004. Statistical properties of local active galactic nuclei inferred from the RXTE 3-20 keV all-sky survey. A&A 423, 469–480.
Sazonov, S.Y., Revnivtsev, M.G., Lutovinov, A.A., Sunyaev, R.A., Grebenev, S.A., 2004. Broadband X-ray spectrum of GRS 1734-292, a luminous Seyfert 1 galaxy behind the Galactic Center. A&A 421, L21–L24.
Semena, A.N., Sazonov, S.Y., Krivonos, R.A., 2019. Spectral Properties of Heavily Obscured Seyfert Galaxies from the INTEGRAL All-Sky Survey. Astronomy Letters 45 (8), 490–520. https://doi.org/10.1134/S1063773719080085.
Sinha, A., Shukla, A., Misra, R., Chitnis, V.R., Rao, A.R., Acharya, B.S., 2015. Underlying particle spectrum of Mkn 421 during the huge X-ray flare in April 2013. A&A 580, A100.
Smith, P.S., Elston, R., Berriman, G., Allen, R.G., Balonek, T.J., 1988. Evidence for Accretion Disks in Highly Polarized Quasars. ApJ 326, L39. https://doi.org/10.1086/185119.
Soldi, S., Beckmann, V., Bassani, L., Courvoisier, T.J.-L., Landi, R., Malizia, A., Dean, A.J., de Rosa, A., Fabian, A.C., Walter, R., 2006. INTEGRAL Observations of Six AGN in the Galactic Plane. In: Wilson, A. (Ed.), The X-ray Universe 2005. ESA Special Publication 604. pp. 667.
Soldi, S., Türler, M., Paltani, S., Aller, H.D., Aller, M.F., Burki, G., Chernyakova, M., Lähteenmäki, A., McHardy, I.M., Robson, E.I., 2008. The multiwavelength variability of 3C 273. A&A 486 (2), 411–425.
Steffen, A.T., Barger, A.J., Cowie, L.L., Mushotzky, R.F., Yang, Y., 2003. The Changing Active Galactic Nucleus Population. ApJ 596 (1), L23–L26.
Stephen, J.B., Bassani, L., Molina, M., Malizia, A., Bazzano, A., Ubertini, P., Dean, A.J., Bird, A.J., Lebrun, F., Much, R., Walter, R., 2005. Using the ROSAT Bright Source Catalogue to find counterparts for IBIS/ISGRI survey sources. A&A 432 (2), L49–L52.
Subrahmanyan, R., Saripalli, L., Hunstead, R.W., 1996. Morphologies in megaparsec-size powerful radio galaxies. MNRAS 279 (1), 257–274.
The Fermi-LAT collaboration, 2019. The Fourth Catalog of Active Galactic Nuclei Detected by the Fermi Large Area Telescope. arXiv e-prints. arXiv:1905.10771
Ubertini, P., Sguera, V., Stephen, J.B., Bassani, L., Bazzano, A., Bird, A.J., 2009. The Fermi/LAT Sky as Seen by INTEGRAL/IBIS. ApJ 706 (1), L7–L11. https://doi.org/10.1088/0004-637X/706/1/L7.
Ueda, Y., Akiyama, M., Hasinger, G., Miyaji, T., Watson, M.G., 2014. Toward the Standard Population Synthesis Model of the X-Ray Background: Evolution of X-Ray Luminosity and Absorption Functions of Active Galactic Nuclei Including Compton-thick Populations. ApJ 786 (2), 104.
Ueda, Y., Akiyama, M., Ohta, K., Miyaji, T., 2003. Cosmological Evolution of the Hard X-Ray Active Galactic Nucleus Luminosity Function and the Origin of the Hard X-Ray Background. ApJ 598 (2), 886–908.
Urry, C.M., Padovani, P., 1995. Unified schemes for radio-loud active galactic nuclei. Publications of the Astronomical Society of the Pacific 107, 803.
Ursini, F., Bassani, L., Panessa, F., Bazzano, A., Bird, A.J., Malizia, A., Ubertini, P., 2018. Where are Compton-thick radio galaxies? A hard X-ray view of three candidates. MNRAS 474 (4), 5684–5693.
Ursini, F., Bassani, L., Panessa, F., Bird, A.J., Bruni, G., Fiocchi, M., Malizia, A., Saripalli, L., Ubertini, P., 2018. Hard X-ray-selected giant radio galaxies - I. The X-ray properties and radio connection. MNRAS 481 (3), 4250–4260.
Vercellone, S., Striani, E., Vittorini, V., Donnarumma, I., Pacciani, L., Pucella, G., Tavani, M., Raiteri, C.M., Villata, M., Romano, P., Fiocchi, M., Bazzano, A., Bianchin, V., Ferrigno, C., Maraschi, L., Pian, E., Türler, M., Ubertini, P., Bulgarelli, A., Chen, A.W., Giuliani, A., Longo, F., Barbiellini, G., Cardillo, M., Cattaneo, P.W., Del Monte, E., Evangelista, Y., Feroci, M., Ferrari, A., Fuschino, F., Gianotti, F., Giusti, M., Lazzarotto, F., Pellizzoni, A., Piano, G., Pilia, M., Rapisarda, M., Rappoldi, A., Sabatini, S., Soffitta, P., Trifoglio, M., Trois, A., Giommi, P., Lucarelli, F., Pittori, C., Santolamazza, P., Verrecchia, F., Agudo, I., Aller, H.D., Aller, M.F., Arkharov, A.A., Bach, U., Berdyugin, A., Borman, G.A., Chigladze, R., Efimov, Y.S., Efimova, N.V., Gómez, J.L., Gurwell, M.A., McHardy, I.M., Joshi, M., Kimeridze, G.N., Krajci, T., Kurtanidze, O.M., Kurtanidze, S.O., Larionov, V.M., Lindfors, E., Molina, S.N.,

Morozova, D.A., Nazarov, S.V., Nikolashvili, M.G., Nilsson, K., Pasanen, M., Reinthal, R., Ros, J.A., Sadun, A.C., Sakamoto, T., Sallum, S., Sergeev, S.G., Schwartz, R.D., Sigua, L.A., Sillanpää, A., Sokolovsky, K.V., Strelnitski, V., Takalo, L., Taylor, B., Walker, G., 2011. The Brightest Gamma-Ray Flaring Blazar in the Sky: AGILE and Multi-wavelength Observations of 3C 454.3 During 2010 November. ApJ 736 (2), L38.

Weżgowiec, M., Jamrozy, M., Mack, K.H., 2016. 1.4-GHz Observations of Extended Giant Radio Galaxies. Acta Astron. 66 (1), 85–119.

Woo, J.-H., Cho, H., Gallo, E., Hodges-Kluck, E., Le, H.A.N., Shin, J., Son, D., Horst, J.C., 2019. A 10,000-solar-mass black hole in the nucleus of a bulgeless dwarf galaxy. Nature Astronomy.

Zdziarski, A.A., 1998. Hot accretion discs with thermal comptonization and advection in luminous black hole sources. Monthly Notices of the Royal Astronomical Society 296 (4), L51–L55.

Zurita Heras, J.A., Chaty, S., Tomsick, J.A., 2009. Infrared identification of igr j09026-4812 as a seyfert 1 galaxy. Astronomy & Astrophysics 502 (3), 787–790.

Angela Malizia graduated with a degree in Astronomy from Bologna University (IT). She then obtained a Ph.D. from Southampton University with a thesis on the high energy properties of Active Galactic Nuclei (AGN). She worked as Archive Manager for the Italian Space Agency during the BeppoSAX mission. From the beginning of the INTEGRAL mission she worked on the IBIS data analysis, in particular on All-Sky Surveys and high energy studies of AGN. She has served in the Target Allocation Committee of INTEGRAL as well as she is currently a member of the INTEGRAL User Group. Her expertise in soft and hard X-ray data analysis and their interpretation are well documented in a more than 110 refereed papers